



## OPEN ACCESS

## EDITED BY

Jeffrey Miecznikowski,  
University at Buffalo, United States

## REVIEWED BY

Haoxiang Cheng,  
Icahn School of Medicine at Mount Sinai,  
United States  
Jinchao Hou,  
Washington University in St. Louis,  
United States

## \*CORRESPONDENCE

Xiaofeng Huang,  
✉ huangxf1998@163.com  
Gerhard Schmalz,  
✉ Gerhard.Schmalz@medizin.uni-  
leipzig.de

<sup>†</sup>These authors have contributed equally  
to this work

RECEIVED 27 June 2023

ACCEPTED 22 September 2023

PUBLISHED 02 October 2023

## CITATION

Jin J, Guang M, Li S, Liu Y, Zhang L,  
Zhang B, Cheng M, Schmalz G and  
Huang X (2023), Immune-related  
signature of periodontitis and Alzheimer's  
disease linkage.  
*Front. Genet.* 14:1230245.  
doi: 10.3389/fgene.2023.1230245

## COPYRIGHT

© 2023 Jin, Guang, Li, Liu, Zhang, Zhang,  
Cheng, Schmalz and Huang. This is an  
open-access article distributed under the  
terms of the [Creative Commons  
Attribution License \(CC BY\)](https://creativecommons.org/licenses/by/4.0/). The use,  
distribution or reproduction in other  
forums is permitted, provided the original  
author(s) and the copyright owner(s) are  
credited and that the original publication  
in this journal is cited, in accordance with  
accepted academic practice. No use,  
distribution or reproduction is permitted  
which does not comply with these terms.

# Immune-related signature of periodontitis and Alzheimer's disease linkage

Jieqi Jin<sup>1†</sup>, Mengkai Guang<sup>2†</sup>, Simin Li<sup>3</sup>, Yong Liu<sup>1</sup>, Liwei Zhang<sup>1</sup>,  
Bo Zhang<sup>1</sup>, Menglin Cheng<sup>1</sup>, Gerhard Schmalz<sup>4\*</sup> and  
Xiaofeng Huang<sup>1\*</sup>

<sup>1</sup>Department of Stomatology, Beijing Friendship Hospital, Capital Medical University, Beijing, China, <sup>2</sup>Department of Stomatology, China-Japan Friendship Hospital, Beijing, China, <sup>3</sup>Stomatological Hospital, Southern Medical University, Guangzhou, China, <sup>4</sup>Department of Cariology, Endodontology and Periodontology, Leipzig University, Leipzig, Germany

**Background:** Periodontitis (PD) and Alzheimer's disease (AD) are both associated with ageing and clinical studies increasingly evidence their association. However, specific mechanisms underlying this association remain undeciphered, and immune-related processes are purported to play a significant role. The accrual of publicly available transcriptomic datasets permits secondary analysis and the application of data-mining and bioinformatic tools for biological discovery.

**Aim:** The present study aimed to leverage publicly available transcriptomic datasets and databases, and apply a series of bioinformatic analysis to identify a robust signature of immune-related signature of PD and AD linkage.

**Methods:** We downloaded gene-expression data pertaining PD and AD and identified crosstalk genes. We constructed a protein-protein network analysis, applied immune cell enrichment analysis, and predicted crosstalk immune-related genes and infiltrating immune cells. Next, we applied consensus cluster analysis and performed immune cell bias analysis, followed by LASSO regression to select biomarker immune-related genes.

**Results:** The results showed a 3 gene set comprising of DUSP14, F13A1 and SELE as a robust immune-related signature. Macrophages M2 and NKT, B-cells, CD4<sup>+</sup> memory T-cells and CD8<sup>+</sup> naive T-cells emerged as key immune cells linking PD with AD.

**Conclusion:** Candidate immune-related biomarker genes and immune cells central to the association of PD with AD were identified, and merit investigation in experimental and clinical research.

## KEYWORDS

Alzheimer's disease, periodontitis, neuroinflammation, multimorbidity, immune pathways, gene expression signature

## Introduction

With the rapid ageing of global populations, the burden of Alzheimer's disease (AD) is rising. AD is a neurodegenerative disease marked by the formation of amyloid- $\beta$  peptide (A $\beta$ P) plaques aggregate in brain tissues. Inflammation and pathological aberrations in central and peripheral immune responses are implicated in AD (Campbell and Gear, 1995; Bettcher et al., 2021). While the relationship of systemic or peripheral inflammation with AD

has been inconsistent (Eriksson et al., 2011), accruing research has highlighted the role of peripheral inflammation in AD pathogenesis. Gut microbiome dysbiosis is associated with neuroinflammation and synaptic dysfunction characteristic of AD (Bairamian et al., 2022). Research using a murine model of AD has demonstrated that low-grade peripheral inflammation is capable of aggravating brain pathology (Xie et al., 2021). ApoE4 allele of the Apolipoprotein E gene, a well-known genetic risk factor of AD, when coupled with chronic low-grade peripheral inflammation leads to earlier onset and greater morbidity from AD (Tao et al., 2018). Peripheral inflammation also alters the connectivity of large-scale cognitive networks in older individuals, particularly in ApoE4 carriers (Walker et al., 2020). Elevated levels of both peripheral and CSF inflammatory markers are associated with AD (Shen et al., 2019). Systemic infections are associated with enhanced immunosuppressive processes in the brains of patients with AD, with an increase in anti-inflammatory proteins including IL4R and CHI3L1 and a decrease in certain proinflammatory proteins, along with lowered T-cell recruitment (Rakic et al., 2018). Systemic inflammation can affect intra-brain drug distribution by altering ABCB1 and ABCG2 protein expression and can also perturb GluN1 protein expression in AD affected brains (Puris et al., 2021). Circulating IL-21, a key immunomodulatory cytokine is elevated in AD, possibly due to immune activation, resulting in neuroinflammation, microglial activation, and deposition of A $\beta$  plaques (Agrawal et al., 2022).

Ageing is associated with higher levels of chronic inflammation and immune deregulation. Infections cause immune dysregulation, an increase circulating pro-inflammatory mediators such as TNF $\alpha$  and IL-6 along with the brain levels of IL-1 $\beta$  and IL-6 levels, aggravating neuroinflammation and accelerating cognitive decline in older adults (Holmes et al., 2011; Lopez-Rodriguez et al., 2021). Immune perturbation in AD is not restricted to the central nervous system (CNS), and peripheral immune dysregulation appears to affect homeostasis in AD-affected brains, where the barrier function is disrupted, allowing an ingress of T-cells (van Olst et al., 2022). Perturbed naive and memory CD4<sup>+</sup> T cell subsets have been noted in the peripheral blood of patients with mild AD and dementia, with a lower proportion of naive cells and an increased proportion of effector memory and terminal differentiation effector memory (TEMRA) CD4<sup>+</sup> cells (McManus et al., 2015). The deregulation of both the peripheral and central immune compartments marks AD. Peripheral immune activation is associated with neuroinflammation and AD pathogenesis. Sustained activation of the brain's microglia and other immune cells is found to exacerbate both amyloid and tau pathology and may serve as the link between infections, chronic peripheral inflammation and AD (Kinney et al., 2018).

Periodontitis is a highly prevalent oral infectious disease that imposes both oral and systemic health burdens. It is an inflammatory disease caused by a complex interplay between dental plaque microbes and the host immune system (Hajishengallis, 2014a). The deposition of a microbial plaque biofilm initiates immune cell migration, and its dysbiosis sustains a local inflammatory response (Murakami et al., 2018). Key periodontal pathogens such as *Porphyromonas gingivalis* are immune evasive and can activate the complement system and pathogen recognition receptors such as TLRs, leading to chronic

**TABLE 1** Statistical analysis of periodontitis and Alzheimer's disease samples.

| Disease | Datasets  | Platform | Case | Control | Total |
|---------|-----------|----------|------|---------|-------|
| PD      | GSE10334  | GPL570   | 241  | 69      | 310   |
|         | GSE16134  | GPL570   | 183  | 64      | 247   |
|         | GSE106090 | GPL21827 | 6    | 6       | 12    |
| AD      | GSE33000  | GPL4372  | 310  | 157     | 467   |
|         | GSE36980  | GPL6244  | 33   | 47      | 80    |
|         | GSE122063 | GPL16699 | 56   | 44      | 100   |
|         | GSE48350  | GPL570   | 80   | 173     | 253   |
|         | GSE5281   | GPL570   | 87   | 74      | 161   |

inflammation and periodontal tissue destruction (Xu et al., 2021). Virulence factors like *Porphyromonas gingivalis* fimbriae can activate TLR2 expressed by innate immune cells (Maekawa et al., 2014), leading to a cascade of cellular and humoral immune responses, and induction of adaptive immune responses (Hajishengallis, 2014a). Ageing is associated with a steep increase in the incidence and severity of periodontitis, attributed in part to increased susceptibility from age-dependent alterations in host innate immunity and inflammatory status (Hajishengallis, 2014b). Cellular senescence, stem cell failure, and immune senescence inherent to biological ageing impair periodontal tissue homeostasis and contribute to the pathophysiology of periodontitis (Baima et al., 2022).

Evidence showing the association of AD with periodontitis is rapidly accumulating (Dominy et al., 2019; Dioguardi et al., 2020; Hu et al., 2021). *Porphyromonas gingivalis* has been found to infiltrate the brains of tissue in AD and is proposed to be an important mechanistic link between periodontitis and AD (Ryder, 2020). Periodontitis also causes widespread systemic immune dysfunction, showing heightened pro-inflammatory responses to *Porphyromonas gingivalis* and attenuated T-cell responses (Gaudilliere et al., 2019). In the present study, we aimed to identify immunological perturbations and immune crosstalk potentially linking periodontitis with AD by leveraging gene expression data.

## Materials and methods

### Gene expression datasets

We downloaded gene expression profile datasets related to periodontitis (PD) and Alzheimer's disease (AD) from the GEO (<https://www.ncbi.nlm.nih.gov/geo/>) database. For PD, we chose gingival tissue and for AD, we chose brain tissue data. The datasets are listed in Table 1.

### Differential gene expression analysis

First, we converted the probe names into gene names based on the downloaded data. If the same gene had multiple expression



values in the same sample, we obtained the mean of the expression values. As differences existed between the datasets, we first combined the datasets for AD and PD each based on common genes, and then applied the “ComBat” method in the R package “SVA” for batch correction. Among the datasets related to AD, since the series matrix of GSE33000 was a standardised dataset, the other four datasets were standardised separately. We then combined the 5 standardised datasets and applied the “ComBat” method to perform batch correction.

Differential expression gene analysis of the corrected datasets was performed using the R package “limma”. For the AD datasets, we used a threshold of  $p$ -value  $< 0.05$ , with  $|\log_2(\text{FC})| > 0$  for upregulated genes and  $\log_2(\text{FC}) < 0$  for downregulated genes. For PD datasets we used  $p$ -value  $< 0.05$ ,  $\log_2(\text{FC}) \geq 0.5$  for upregulated genes and  $\log_2(\text{FC}) < = 0.5$  for downregulated genes.

## Identification of crosstalk genes

The differentially expressed genes of AD and PD were intersected and the shared genes were regarded as potential crosstalk genes. Functional enrichment analysis of the crosstalk genes was performed using “clusterProfiler” (GO Biological processes and KEGG pathways, at a threshold of  $p$ -value  $< 0.05$ ).

## Crosstalk genes’ protein-protein interaction (PPI) network analysis

We downloaded protein-protein related gene pairs from MINT (<http://mint.bio.uniroma2.it/mint/Welcome.do>), HPRD ([http://www.hprd.org/index\\_html](http://www.hprd.org/index_html)), BIOGRID (<http://thebiogrid.org/>), DIP (<http://dip.doe-mbi.ucla.edu/dip/Main.cgi>), mentha (<http://mentha.uniroma2.it/index.php>), PINA (<http://cbg.garvan.unsw.edu.au/pina/>), InnateDB (<http://www.innatedb.com/>), and Instruct (<http://instruct.yulab.org/index.html>) databases. Next, PPI relationship pairs for the crosstalk genes were extracted, and a PPI network was constructed using Cytoscape software, with the plug-in “NetworkAnalyzer” to analyse the network’s topological properties.

## Crosstalk genes’ immune cell enrichment analysis

XCell (<https://xcell.ucsf.edu/>) was used for cell type enrichment of the crosstalk genes. XCell includes 64 cell types involving multiple adaptive and innate immune cells, hematopoietic progenitors, epithelial cells, and extracellular matrix cells, comprising 48 tumor microenvironment-related cells. We first extracted Case

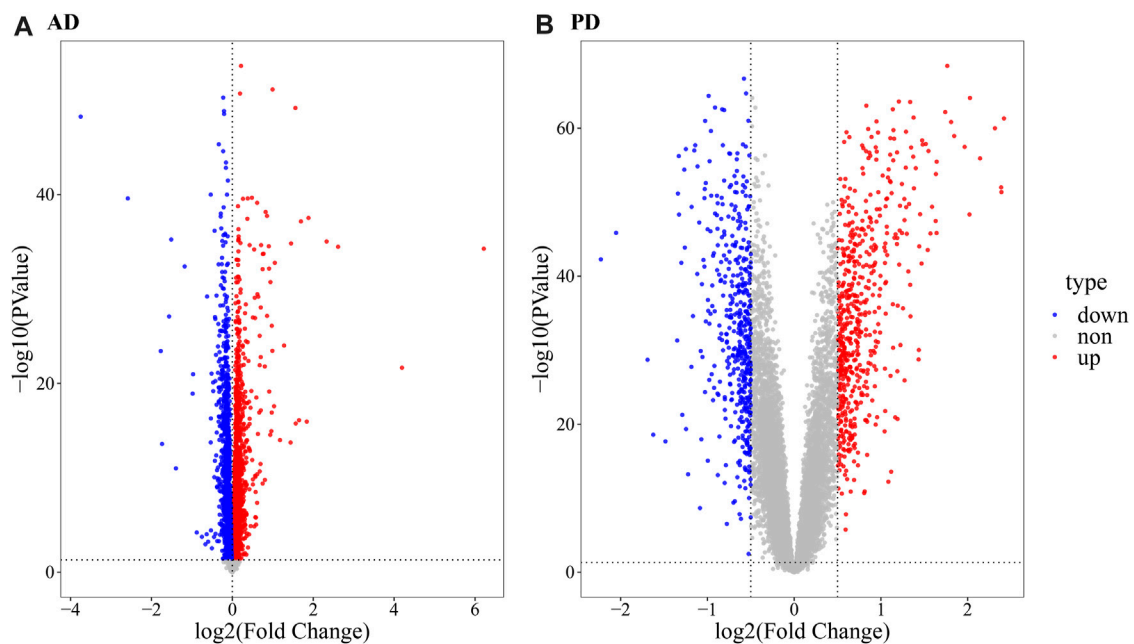


**FIGURE 2**

Volcano map depicting differentially expressed genes. **(A)** Volcano map of differentially expressed genes in AD; **(B)** Volcano map of differentially expressed genes in PD. The R package “limma” was used for differential gene expression analysis. For the AD datasets, a threshold of  $p$ -value  $< 0.05$ ,  $|\log_2(\text{FC})| > 0$  for upregulated genes and  $\log_2(\text{FC}) < 0$  for downregulated genes was used. For PD datasets, a  $p$ -value  $< 0.05$ ,  $\log_2(\text{FC}) \geq 0.5$  for upregulated genes and  $\log_2(\text{FC}) < -0.5$  for downregulated genes was used.

samples from AD and PD datasets and obtained the expression values of crosstalk genes. The gene number limit for the raw enrichment analysis method in the xCell package was reset and the scores for immune-infiltrating cells corresponding to the samples were calculated. Next, “transform scores” and “spill over” were used to obtain the final corrected immune infiltrating cell scores.

## Analysis of immune-related genes and infiltrating immune cells

Immune-related genes were downloaded from an earlier publication (Charoentong et al., 2017) (782 genes, including 431 genes related to 15 adaptive immune cell types and 351 genes related to 13 innate immune cell types) and combined with immune-related genes from Innate DB (<https://innatedb.com/annotatedGenes.do?type=innatedb>) and ImmPort (<https://www.immport.org/home>) datasets. The expression values of these immune-related genes in the AD and PD case samples were extracted and the xCell algorithm was used to obtain the expression scores of infiltrating immune cells. The differences between the immune cell fractions in the two diseases was tested using the Wilcoxon’s test ( $p < 0.05$ ).

## Consensus cluster analysis of AD and PD samples based on immune-related genes

We applied consensus clustering to the expression matrix profiles of immune-related genes in AD and PD each, using the

“ConsensusClusterPlus” package. Average silhouette width, gap statistic, and the elbow method were used to determine the optimal number of clusters. Next, the samples were clustered using clustering consistency.

## Adaptive and innate immune cell bias analysis

We combined the immune cell fractions and sample clusters of case samples from AD and PD. For each consensus cluster, statistics for cluster distribution of xCell scores for adaptive and innate immune-related genes were computed. The difference between scores of immune cells in different clusters was tested using the Kruskal Wallis test. We also noted the overall scores of immune cells in different clusters to determine immune cells that characterized a cluster.

## Identification of potential biomarkers using LASSO logistic regression

We extracted the expression values of the crosstalk genes for the case and control groups and applied LASSO logistic regression. From the screened crosstalk genes, those common to AD and PD were considered biomarker crosstalk genes. Next, adaptive immune cell-related genes were identified based on the literature, and their expression profiles in AD and PD datasets were screened using LASSO logistic regression. The intersecting genes were recorded as biomarker adaptive immune genes. For Innate immune cell-related

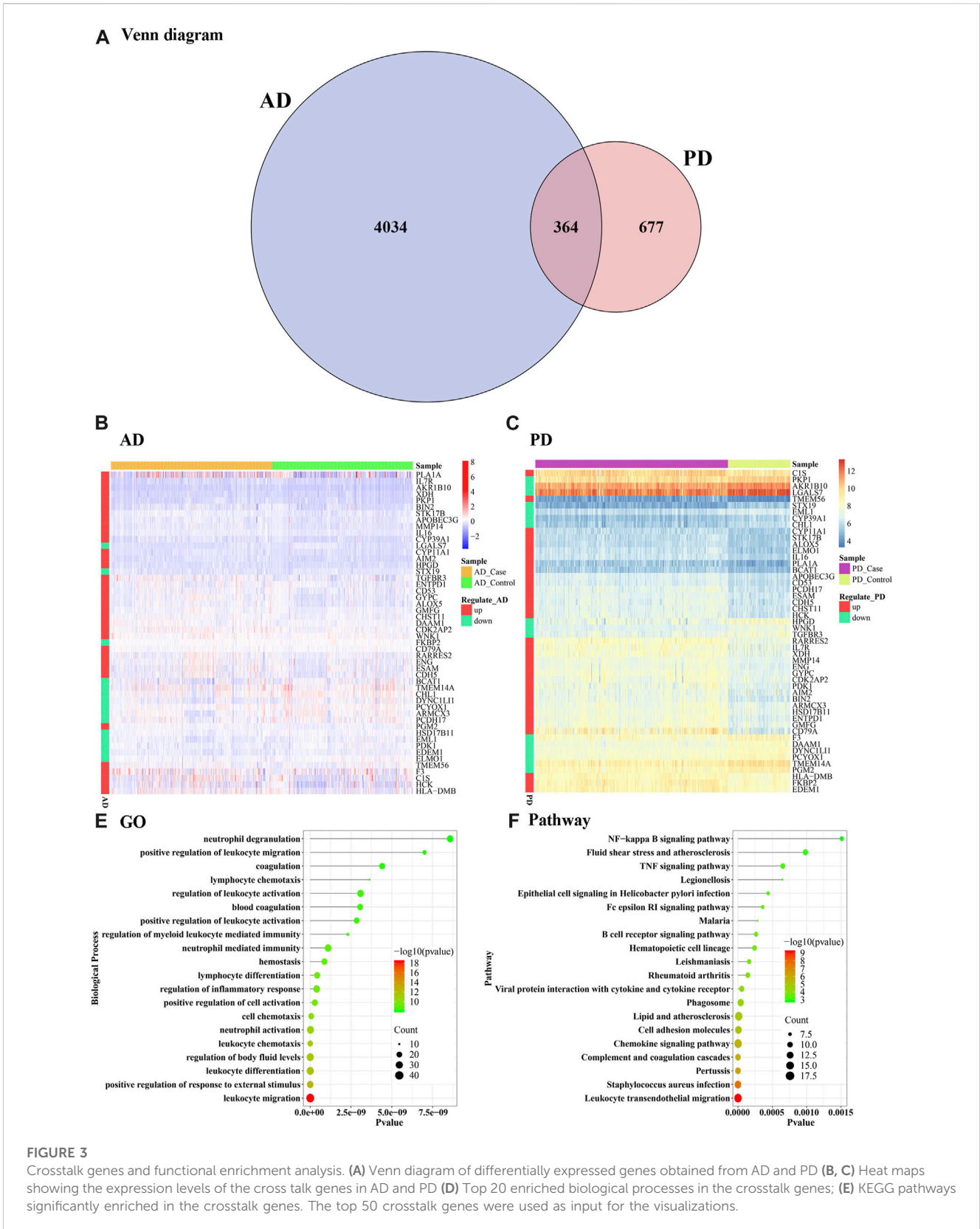
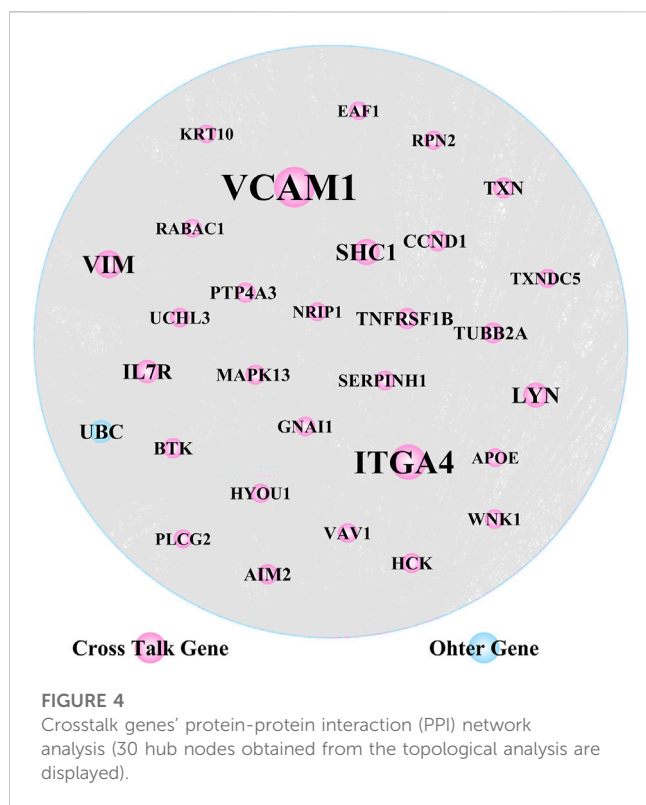


**FIGURE 3** Crosstalk genes and functional enrichment analysis. (A) Venn diagram of differentially expressed genes obtained from AD and PD (B, C) Heat maps showing the expression levels of the cross talk genes in AD and PD (D) Top 20 enriched biological processes in the cross talk genes; (E) KEGG pathways significantly enriched in the cross talk genes. The top 50 cross talk genes were used as input for the visualizations.

genes, we combined those obtained from literature with those obtained from the InnateDB dataset and obtained 1,335 innate immune-cell related genes. LASSO logistic regression was similarly applied, and biomarker innate immune genes were

identified. In the next step, the intersections of biomarker crosstalk genes with biomarker adaptive immune cell-related genes and biomarker innate immune cell-related genes were determined. Receiver operating curve (ROC) analysis was



performed using these genes' expression values. Human KEGG pathways and related genes were obtained from the KEGG database (<https://www.kegg.jp/>) and pathways that correspond to these intersecting genes were identified and all genes in each such pathway were listed. Interactions between the KEGG pathways, biomarker crosstalk genes, biomarker adaptive immune-cell related genes, and biomarker innate immune cell-related genes were identified.

## Results

### Differentially expressed genes

As evident in Figure 1, significant clustering by batch was noted for both AD and PD gene expression datasets before correction and was reduced post batch correction (Figure 1). Using the batch corrected data, we obtained 4,398 differentially expressed genes in AD and 1,041 differentially expressed genes in PD, respectively. A volcano map was used to display the distribution of the differentially expressed genes (Figure 2).

### Crosstalk genes enrichment in immune related pathways

A total of 364 Crosstalk genes were obtained (Figure 3A) by intersection of the differentially expressed genes of PD and AD. To visualize changes in the expression values of crosstalk genes in different sample types, heat maps were plotted using the "pheatmap" R package, using top 50 Crosstalk genes as the input (Figures 3B, C). To further analyze

the functions of the crosstalk genes functional enrichment analysis was performed and significantly enriched GO Biological process and KEGG Pathways were identified and the top 20 were visualized (Figures 3D–E).

Gene ontology analysis showed that the crosstalk genes mainly regulated several leukocyte functions including chemotaxis, migration, differentiation, and myeloid leukocyte related immunity. In particular, neutrophil activation, degranulation, and associated immunity. Blood coagulation, hemostasis and body fluid balance regulation were also enriched among the crosstalk genes (Figure 3D). Among the enriched KEGG pathways, leukocyte transendothelial migration, *S. aureus* infection, and complement and coagulation cascades showed the top-most significance. Innate immune pathways including chemokine signaling, NF kappa beta signaling, and TNF signaling pathways were noted. Lipid and atherosclerosis pathway, epithelial cell signaling and cell-mediated immune pathway B cell receptor signaling were also notably enriched among others including rheumatoid arthritis, Fc epsilon R1 signaling and viral protein interaction with cytokine receptor (Figure 3E).

### Key crosstalk genes identified through PPI network analysis

We extracted PPI relationship pairs for the 364 crosstalk genes and constructed a PPI network (Figure 4), which showed 4,870 nodes and 9,657 edges. The topological properties of the network were analyzed, and the top 30 hub node genes (Table 2) were identified based on the degree of gene connectivity and considered as the most important genes nodes in the protein interaction network relationship.

VCAM1, ITGA4 and VIM, were noted as the top genes playing an important role in the network, and were upregulated in both AD and PD. Several of the gene nodes showed opposing patterns of regulation in the two diseases. KRT10, WNK1, MAPK13, TUBB2A and CCND1 were upregulated in AD but downregulated in PD. Conversely, RABAC1 and HYOU1 were downregulated in AD but upregulated in PD.

### Immune cell fractions enriched by the crosstalk genes show comparative differences between AD and PD

Using the xCell package, scores of immune-infiltrating cells corresponding to the 364 Crosstalk genes were calculated and "transform scores" and "spillOver" were applied to obtain the final corrected immune cell scores. Scores of 55 immune cell types in the AD and PD datasets were noted and a heatmap was used to display the scores of immune infiltrating cells in AD and PD datasets (Figure 5A).

A violin diagram drawn using "vioplot" was used to depict the scores of each immune infiltrating cell in both diseases (Figures 5B–D). The difference in scores of immune infiltrating cells for the Case samples of AD and PD datasets was tested using Wilcoxon's test. The cells were grouped in three categories and displayed (Figures 5B–D). We can see that several immune cell types are closely related in both diseases. AD samples showed highly significantly higher scores for adipocytes, CD4<sup>+</sup> and CD8<sup>+</sup> T-cell

TABLE 2 Topological characteristics of the top 30 gene nodes in the crosstalk-gene PPI network.

| Name     | AD_PD     | Degree | Average shortest path length | Betweenness centrality | Closeness centrality | Clustering coefficient | Topological coefficient |
|----------|-----------|--------|------------------------------|------------------------|----------------------|------------------------|-------------------------|
| VCAM1    | up_up     | 673    | 2.612737                     | 0.150601               | 0.38274              | 0.002503               | 0.003982                |
| ITGA4    | up_up     | 528    | 2.611707                     | 0.099121               | 0.382891             | 0.003996               | 0.004326                |
| VIM      | up_up     | 320    | 2.645095                     | 0.105724               | 0.378058             | 0.003174               | 0.006497                |
| SHC1     | up_up     | 273    | 2.812861                     | 0.065675               | 0.35551              | 0.005602               | 0.009555                |
| LYN      | up_up     | 243    | 2.731451                     | 0.072094               | 0.366106             | 0.006462               | 0.007585                |
| IL7R     | up_up     | 199    | 2.86892                      | 0.035555               | 0.348563             | 0.002335               | 0.010105                |
| UBC      |           | 184    | 2.253504                     | 0.340648               | 0.443753             | 0.005702               | 0.010612                |
| TXN      | down_down | 132    | 2.796785                     | 0.027568               | 0.357553             | 0.0096                 | 0.011983                |
| TNFRSF1B | up_up     | 131    | 2.958368                     | 0.032291               | 0.338024             | 0.001174               | 0.011297                |
| TUBB2A   | up_down   | 124    | 2.865829                     | 0.030234               | 0.348939             | 0.003278               | 0.012209                |
| CCND1    | up_down   | 121    | 3.020816                     | 0.02919                | 0.331036             | 0.00124                | 0.017982                |
| BTK      | up_up     | 112    | 2.934048                     | 0.022542               | 0.340826             | 0.015766               | 0.017501                |
| AIM2     | up_up     | 109    | 3.370363                     | 0.02737                | 0.296704             | 0                      | 0.016514                |
| PTP4A3   | up_up     | 109    | 3.336974                     | 0.024112               | 0.299673             | 1.70E-04               | 0.017308                |
| MAPK13   | up_down   | 103    | 3.092745                     | 0.013791               | 0.323337             | 0                      | 0.024619                |
| HCK      | up_up     | 100    | 2.968879                     | 0.018268               | 0.336827             | 0.012525               | 0.020322                |
| SERPINH1 | up_up     | 96     | 2.955894                     | 0.020851               | 0.338307             | 0.003728               | 0.017841                |
| VAV1     | up_up     | 95     | 2.930338                     | 0.014357               | 0.341258             | 0.028219               | 0.019849                |
| GNAI1    | down_down | 93     | 3.09357                      | 0.029624               | 0.323251             | 0.001636               | 0.015197                |
| WNK1     | up_down   | 92     | 3.109439                     | 0.022769               | 0.321601             | 4.78E-04               | 0.022952                |
| UCHL3    | down_down | 90     | 3.072135                     | 0.018117               | 0.325507             | 0.002747               | 0.021144                |
| HYOU1    | down_up   | 80     | 3.079555                     | 0.015011               | 0.324722             | 0.001266               | 0.02724                 |
| RPN2     | up_up     | 79     | 3.097486                     | 0.01577                | 0.322843             | 0                      | 0.027241                |
| TXNDC5   | up_up     | 78     | 3.068219                     | 0.019356               | 0.325922             | 0                      | 0.025968                |
| RABAC1   | down_up   | 71     | 3.022465                     | 0.01991                | 0.330856             | 0.002414               | 0.016747                |
| APOE     | up_up     | 70     | 2.906018                     | 0.020983               | 0.344113             | 0.004555               | 0.016556                |
| PLCG2    | up_up     | 69     | 2.955482                     | 0.010744               | 0.338354             | 0.047315               | 0.024349                |
| KRT10    | up_down   | 68     | 2.854699                     | 0.00891                | 0.3503               | 0.04302                | 0.027171                |
| NRIP1    | down_down | 68     | 3.084295                     | 0.015047               | 0.324223             | 0                      | 0.027749                |
| EAF1     | down_down | 67     | 3.571517                     | 0.019232               | 0.279993             | 0.003618               | 0.02098                 |

subsets, cDC and DC cell types. Endothelial cells, mast cells and macrophage cells, along with neutrophils, MSC, Th2, HSC, iDC, plasma cells and pro-B cells were comparatively overexpressed in AD, in particular, M2 macrophage cells. Chondrocytes, osteoblasts and fibroblast cells showed greater overexpression in PD.

To test the correlation between immune cells, a correlation analysis of xCell scores for Case samples for each immune cell type in the two data sets was applied (Figures 6A, B).

For AD, immune cell CD8<sup>+</sup> Tem and Th2 cells were highly positively correlated (COR = 0.8196), CD8<sup>+</sup> Tcm and CD8<sup>+</sup> Tem were highly positively correlated (COR = 0.8127), CD8<sup>+</sup> T-cells and

CD8<sup>+</sup> Tcm were highly positively correlated (COR = 0.7822). B-cells were highly negatively correlated with Basophils (COR = -0.7763). For PD, CD8<sup>+</sup> Tcm and CD8<sup>+</sup> Tem were highly positively correlated (cor = 0.9695), Tgd cells and Th2 cells were highly positively correlated (cor = 0.9657), CD8<sup>+</sup> Tem and Tgd cells were highly positively correlated (0.9500), CD8<sup>+</sup> Tem and Th2 cells were highly positively correlated (cor = 0.8954). MSC and Preadipocytes were highly negatively correlated (cor = -0.7754), CD4<sup>+</sup> memory T-cells and Pericytes were highly negatively correlated (cor = -0.7173), Memory B-cells and pro B-cells were highly negatively correlated (cor = -0.6979).

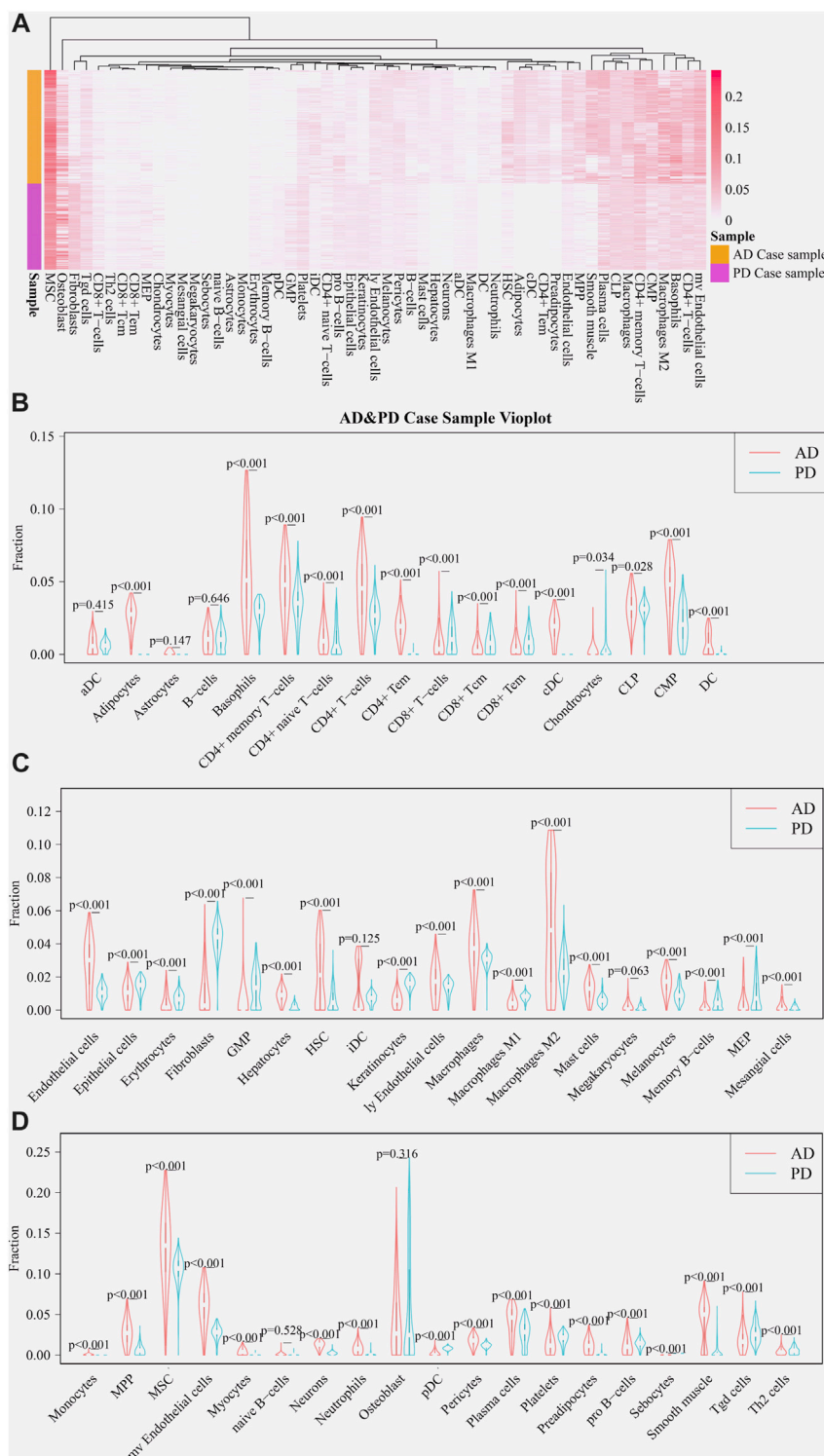


**FIGURE 5** Expression of immune cells in AD and PD. **(A)** Thermographic representation of immune cell expression scores in AD and PD. **(B–D)** Violin diagram of immune cells expression scores in AD and PD. The “xCell” package was used to obtain scores of 55 immune infiltrating cells in both disease sample datasets and differences were tested using Wilcoxon’s analysis.

### Immune-related genes and immune cells enriched in AD and PD

The immune-related genes downloaded from the literature included genes related to 15 Adaptive immune cell and 13 Innate

immune cell types (Figure 7A). Further immune-related genes were obtained from InnateDB and ImmPort databases. We merged the immune-related genes acquired from literature, InnateDB, and ImmPort databases to obtain 3,046 immune genes as the final immune-related gene dataset. We extracted

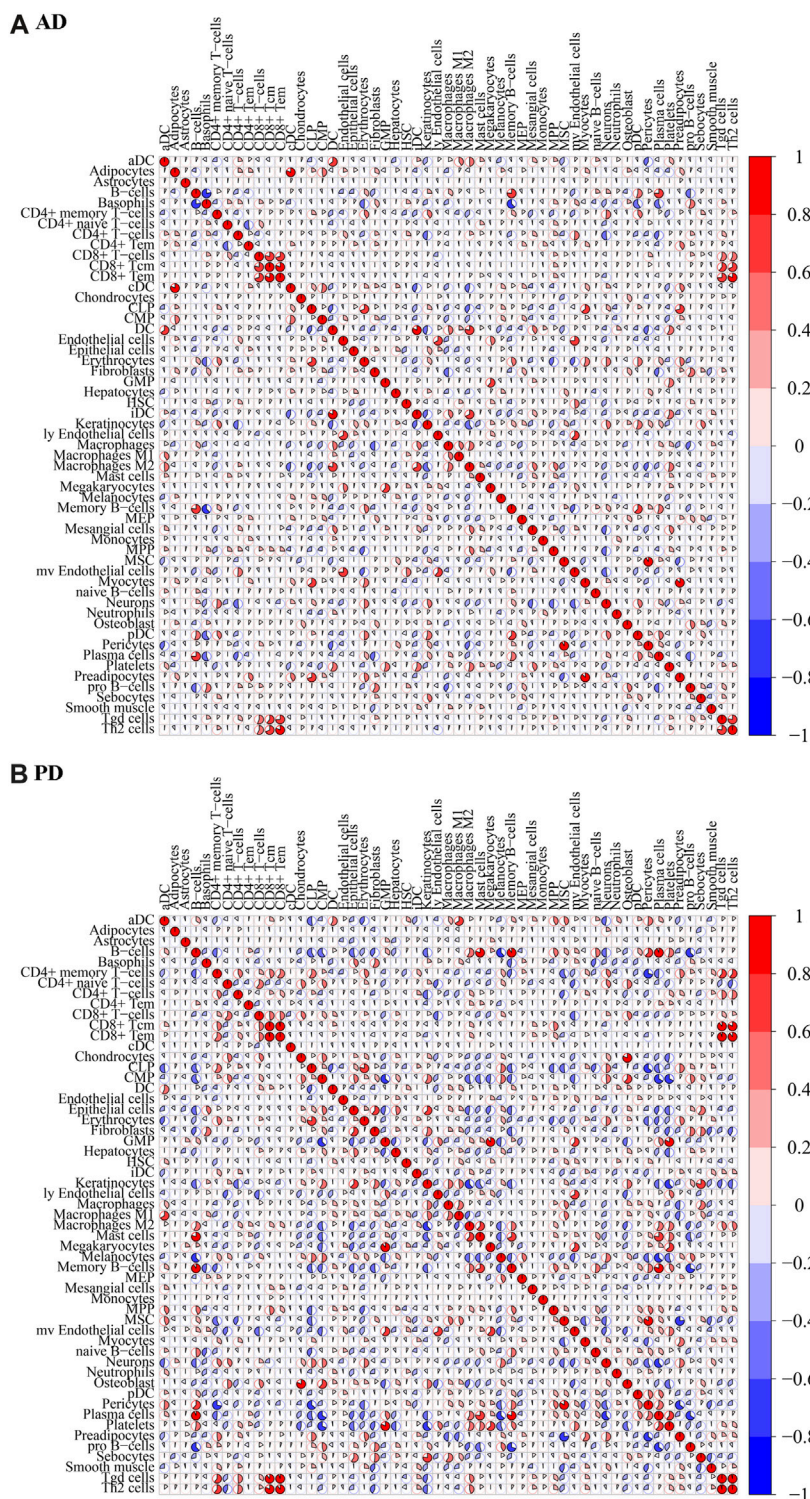


**FIGURE 6**  
Correlation of immune cell scores in Case groups of (A) AD and (B) PD. xCell scores for each immune cell type in the case samples were subjected to Spearman's correlation analysis.

the expression values of these 3,046 immune genes in the Case samples of AD and PD and found that 1,142 immune genes were expressed in AD whereas 2,396 immune genes were expressed in PD. Using the xCell algorithm, we obtained the expression scores

of immune cells in the Case samples of AD and PD. Since the names of 64 cell types included in xCell were different from the names of 28 cell types listed in literature, we identified and listed the cell types (Table 3).

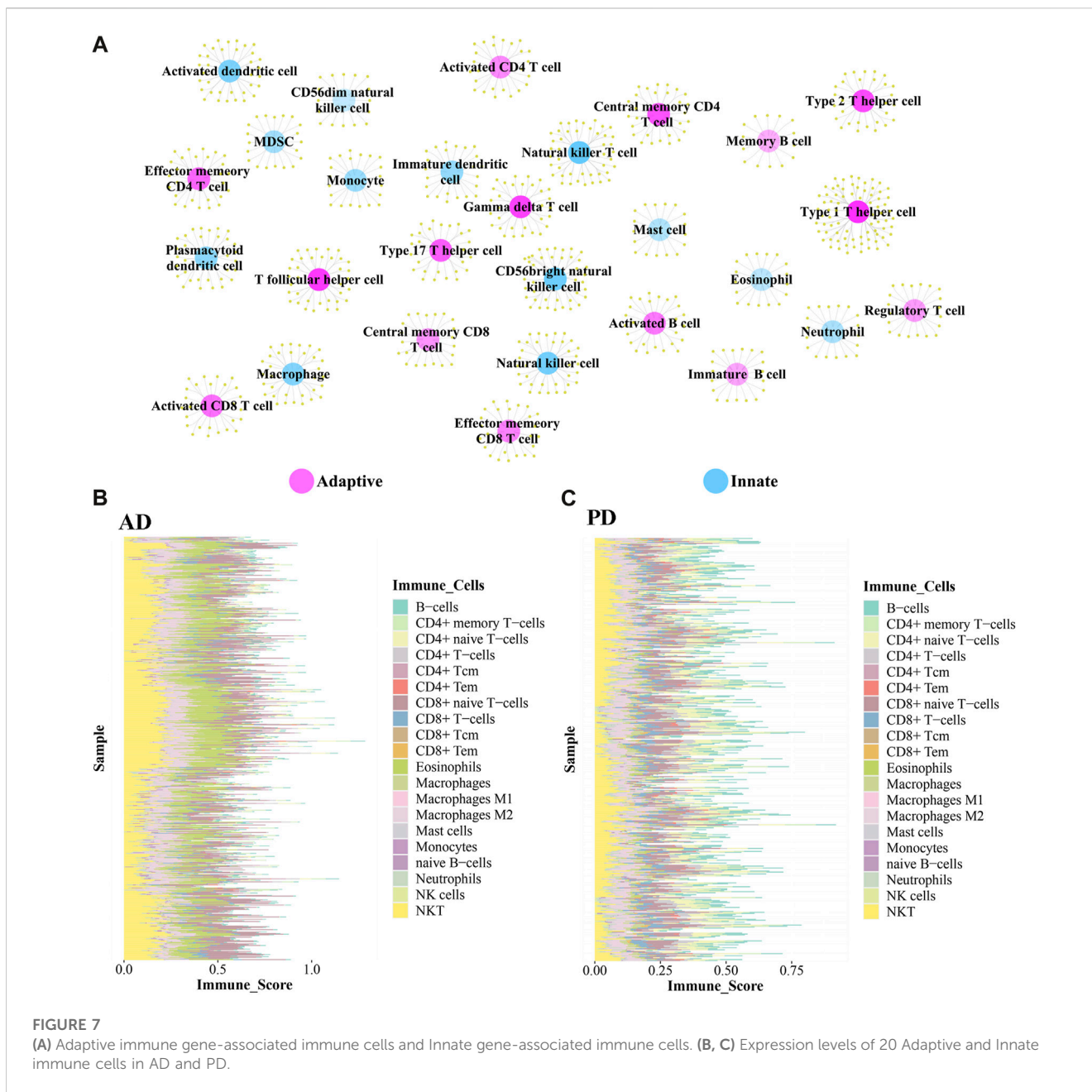


**FIGURE 7**

(A) Adaptive immune gene-associated immune cells and Innate gene-associated immune cells. (B, C) Expression levels of 20 Adaptive and Innate immune cells in AD and PD.

10 adaptive and 10 innate immune cell types were noted in xCell and are marked with different colors. These 20 cell types were extracted for subsequent analysis and their scores were analysed. The fraction of these immune cells is depicted in Figure 7B.

Among the adaptive immune cells, most cells showed higher expression in AD, while CD4<sup>+</sup> naive T-cells and B-cells were highly expressed in PD samples as compared with AD samples. The expression of Eosinophils was higher in AD disease samples than in PD disease samples. Macrophages M2, Natural killer T cell (NKT) and CD8<sup>+</sup> naive T-cells were highly expressed in AD and PD samples. Macrophages M2 and Natural killer T cell (NKT) are innate immune cells, while CD8<sup>+</sup> naive T-cells are adaptive.

A violin diagram was drawn to depict the scores of each immune infiltrating cell in both diseases (Figure 8A) and differences between AD and PD datasets were tested using Wilcoxon's test ( $p < 0.05$ ).

Macrophages M2, Natural killer T cell (NKT) and CD8<sup>+</sup> naive T-cells were found to be significantly different in AD and PD. Then, we examined the correlation between the 20 immune cells in AD and PD (Figures 8B, C). CD8<sup>+</sup> T-cells and CD8<sup>+</sup> naive T-cells, CD4<sup>+</sup> memory T-cells and CD4<sup>+</sup> T-cells were highly positively correlated in AD and PD (Table 4).

### Consensus cluster analysis of immune cells based on immune genes

1,142 immune genes found expressed in AD and 2,396 immune genes found expressed in PD were subjected to Consensus Clustering. The maxK values were determined using average silhouette width, gap statistic, and the elbow method to find the

**TABLE 3 Common immune cells xCell and literature (Charoentong et al., 2017).**

| [xCell] cells 1                 | [xCell] cells 2      | [Charoentong et al., 2017]Cells | [Charoentong et al., 2017] cells immunity |
|---------------------------------|----------------------|---------------------------------|---|
| aDC                             | iDC                  | Activated B cell                | Adaptive                                  |
| Adipocytes                      | Keratinocytes        | Activated CD4 T cell            | Adaptive                                  |
| Astrocytes                      | ly Endothelial cells | Activated CD8 T cell            | Adaptive                                  |
| B-cells                         | Macrophages          | Central memory CD4 T cell       | Adaptive                                  |
| Basophils                       | Macrophages M1       | Central memory CD8 T cell       | Adaptive                                  |
| CD4 <sup>+</sup> memory T-cells | Macrophages M2       | Effector memeory CD4 T cell     | Adaptive                                  |
| CD4 <sup>+</sup> naive T-cells  | Mast cells           | Effector memeory CD8 T cell     | Adaptive                                  |
| CD4 <sup>+</sup> T-cells        | Megakaryocytes       | Gamma delta T cell              | Adaptive                                  |
| CD4 <sup>+</sup> Tcm            | Melanocytes          | Immature B cell                 | Adaptive                                  |
| CD4 <sup>+</sup> Tem            | Memory B-cells       | Memory B cell                   | Adaptive                                  |
| CD8 <sup>+</sup> naive T-cells  | MEP                  | Regulatory T cell               | Adaptive                                  |
| CD8 <sup>+</sup> T-cells        | Mesangial cells      | T follicular helper cell        | Adaptive                                  |
| CD8 <sup>+</sup> Tcm            | Monocytes            | Type 1 T helper cell            | Adaptive                                  |
| CD8 <sup>+</sup> Tem            | MPP                  | Type 17 T helper cell           | Adaptive                                  |
| cDC                             | MSC                  | Type 2 T helper cell            | Adaptive                                  |
| Chondrocytes                    | mv Endothelial cells | Activated dendritic cell        | Innate                                    |
| Class-switched memory B-cells   | Myocytes             | CD56bright natural killer cell  | Innate                                    |
| CLP                             | naive B-cells        | CD56dim natural killer cell     | Innate                                    |
| CMP                             | Neurons              | Eosinophil                      | Innate                                    |
| DC                              | Neutrophils          | Immature dendritic cell         | Innate                                    |
| Endothelial cells               | NK cells             | Macrophage                      | Innate                                    |
| Eosinophils                     | NKT                  | Mast cell                       | Innate                                    |
| Epithelial cells                | Osteoblast           | MDSC                            | Innate                                    |
| Erythrocytes                    | pDC                  | Monocyte                        | Innate                                    |
| Fibroblasts                     | Pericytes            | Natural killer cell             | Innate                                    |
| GMP                             | Plasma cells         | Natural killer T cell           | Innate                                    |
| Hepatocytes                     | Platelets            | Neutrophil                      | Innate                                    |
| HSC                             | Preadipocytes        | Plasmacytoid dendritic cell     | Innate                                    |
| Smooth muscle                   | pro B-cells          |                                 |   |
| Tgd cells                       | Sebocytes            |                                 |   |
| Th1 cells                       | Skeletal muscle      |                                 |   |
| Th2 cells                       | Tregs                |                                 |   |

optimal number of clusters for the AD and PD expression matrices (Figures 9A–F).

As seen in Figure 9, the number of optimal clusters denoted by the three methods were different, which may be related to the large number of gene features and the differences in the algorithms. In AD, the maximum number of clusters was 5 and the minimum number was 2. In PD, the maximum number was 6 and the minimum number was 1. Clustering consistency results for

2-5 clusters in AD, and 2-6 clusters in PD were analysed. Key clustering consistency results for AD and PD are depicted in Figures 10A–F.

The results show that to get the final k value, the descending slope of the Central Line and the relative change of the area under the CDF curve between K and K-1 should be as small as possible. We finally choose K = 4 for AD and PD both. Figure EF shows the correlation between AD and PD samples at the selected k values. The

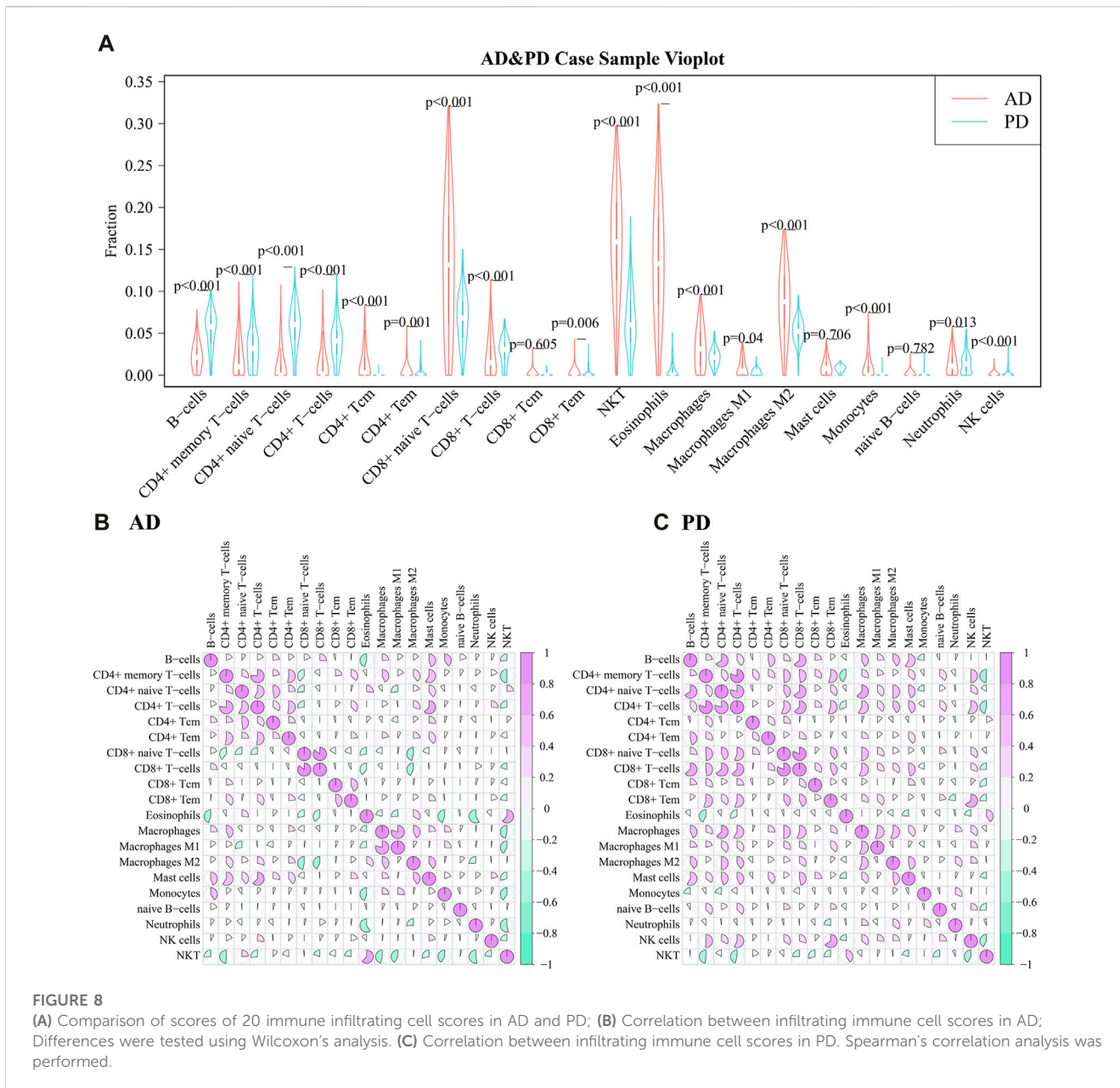


**FIGURE 8** (A) Comparison of scores of 20 immune infiltrating cell scores in AD and PD; (B) Correlation between infiltrating immune cell scores in AD; Differences were tested using Wilcoxon's analysis. (C) Correlation between infiltrating immune cell scores in PD. Spearman's correlation analysis was performed.

rows and columns of the matrix represent the samples. Consistency matrix values are shown in white to dark blue on a scale from 0 (impossible to cluster together) to 1 (always cluster together). The consistency matrix is arranged according to the consistency categories (tree at the top of the heatmap). The bar between the tree and the heat map is the category. The more scattered the dark blue squares, the weaker the clustering results. The cluster-consensus and item-consensus for AD and PD was analysed using the calcICL method in the ConsensusClusterPlus package (Figures 11A–D).

From Figure 11 we can see whether the classification of each sample has sufficient fidelity, to help determine the k value. As shown in Figures 10, 11 we clustered the AD and PD disease samples in 4 clusters each. The sample clustering results and the 20 Adaptive and Innate immune cell scores for AD and PD across all samples are shown (Figure 7B). Next, we combined the immune cell fractions

and sample cluster results for the Case samples from AD and PD for subsequent analysis.

### Adaptive and innate immune cell bias analysis

For each consensus cluster, we calculated the cluster distribution of xCell scores of Adaptive and Innate immune genes in AD and PD and presented these in a box plot (Figures 12A–D). The Kruskal-Wallis test was performed to test differences in scores of immune cells in different clusters.

In Figure 12 we can see that there were significant differences between immune cells in different clusters, and the greater this difference, the more marked the difference between the clusters. We can also see the overall scores of immune cells in different clusters.

**TABLE 4** 20 types of immune cells highly positively correlated (COR  $\geq 0.6$ ) in AD and PD.

| Cell1                           | Cell2                          | PD_cor   | PD_p-value |
|---------------------------------|--------------------------------|----------|------------|
| CD8 <sup>+</sup> naive T-cells  | CD8 <sup>+</sup> T-cells       | 0.81793  | 8.186E-105 |
| CD4 <sup>+</sup> memory T-cells | CD4 <sup>+</sup> T-cells       | 0.801068 | 1.9407E-97 |
| CD4 <sup>+</sup> naive T-cells  | CD4 <sup>+</sup> T-cells       | 0.799333 | 1.0145E-96 |
| B-cells                         | CD4 <sup>+</sup> naive T-cells | 0.660739 | 2.7763E-55 |
| CD8 <sup>+</sup> Tem            | NK cells                       | 0.654085 | 7.5844E-54 |
| CD4 <sup>+</sup> naive T-cells  | CD8 <sup>+</sup> T-cells       | 0.652631 | 1.5451E-53 |
| B-cells                         | CD8 <sup>+</sup> T-cells       | 0.643272 | 1.3744E-51 |
| CD4 <sup>+</sup> T-cells        | CD8 <sup>+</sup> T-cells       | 0.633225 | 1.433E-49  |
| CD4 <sup>+</sup> naive T-cells  | Macrophages                    | 0.628991 | 9.6533E-49 |
| Cell1                           | Cell2                          | AD_cor   | AD_p-value |
| CD8 <sup>+</sup> naive T-cells  | CD8 <sup>+</sup> T-cells       | 0.854951 | 6.467E-163 |
| Macrophages                     | Macrophages M1                 | 0.796427 | 2.673E-125 |
| CD4 <sup>+</sup> memory T-cells | CD4 <sup>+</sup> T-cells       | 0.767739 | 4.144E-111 |
| CD4 <sup>+</sup> T-cells        | Mast cells                     | 0.62343  | 2.8898E-62 |
| Eosinophils                     | NKT                            | 0.620524 | 1.5309E-61 |

The top 3 immune cells from the significant clusters in AD and PD were considered high expression immune cells that play an important role in disease pathology (Table 5).

The results showed that B-cells, CD4<sup>+</sup> memory T-cells and CD8<sup>+</sup> naive T-cells were adaptive immune cells that were highly expressed in all 4 clusters of both diseases, and innate immune cells Macrophages M2 and NKT, were similarly highly expressed in all clusters. Adaptive immune cells CD8<sup>+</sup> naive T- Cells were significantly different between cluster 2 and cluster 3 in AD, and in PD, both.

We extracted the immune-related genes from the Crosstalk gene dataset and obtained 112 genes in total. Then we extracted the expression values of these 112 genes in the Case samples of AD and PD. Correlation analysis was conducted by combining these values with the xCell scores. These two datasets pertaining to each cluster were subjected to correlation analysis. Correlation results were obtained for each of the 8 clusters and are depicted (Figures 13A, B) allowing an estimation of immune cells bias in the different clusters, and also to allow for selection of specific cluster of subjects for longitudinal study.

The results show immune cell biases in different clusters. For adaptive immune-related genes, cluster1 and cluster4 in PD were highly correlated with a variety of immune cells. In cluster2 and cluster3, immune genes were positively correlated with immune cells. Adaptive immune related genes were highly correlated with a variety of immune cells in cluster 4 of AD, and participated in a variety of immune patterns (Figure 13A). For innate immune related genes, multiple immune cells in cluster4 of PD and cluster4 of AD were highly correlated, suggesting that innate genes were more active in cluster4 samples of PD and AD (Figure 13B).

## Candidate biomarkers identified using LASSO logistic regression

Datasets of expression values for Case and Control samples of AD and PD were obtained. The expression values of the crosstalk genes were subjected to LASSO Logistic Regression to screen the crosstalk genes (Figures 14A, B). The intersecting genes were selected and 127 genes were recorded as the candidate biomarker crosstalk genes.

For Adaptive immune-related genes, we extracted 431 genes' expression profiles, which included 210 genes found in AD and 408 genes found in PD datasets and applied LASSO Logistic Regression (Figures 14C, D). The intersecting genes among AD and PD were selected and a total of 78 genes were recorded as the biomarker adaptive immune genes.

For Innate immune genes, we combined the innate immune genes obtained from literature with those obtained from InnateDB data to obtain 1,335 Innate immune genes. 571 such genes were found in AD and 1,183 in PD. LASSO Logistic Regression was applied (Figures 14E, F) and a total of 32 intersecting genes were recorded as biomarker Innate immune gene. A diagram displayed the variation of the remaining variables' gene coefficients with different lambda values from the LASSO regression analysis.

We obtained 3 genes from the intersection of the biomarker crosstalk genes and the biomarker adaptive immune genes, and 1 gene (DEFB1) from the intersection of the biomarker crosstalk genes with the biomarker innate-immune genes. ROC analysis using the expression values of these 4 genes yielded 3 genes (DUSP14, F13A1, SELE) (Figures 15A, B).

AUC (AUC>70%) values obtained for DUSP14, F13A1, SELE and DEFB1 in discriminating PD were higher than those for AD prediction. SELE performed better than the other 3 genes in discriminating both AD and PD. To further analyse the functions of these genes, we obtained datasets of human KEGG pathways and related genes and mined the corresponding pathways, and then isolated all the genes in each pathway. We examined whether there is interaction between each pathway and the biomarker crosstalk genes, biomarker adaptive immune genes, and biomarker innate immune genes (Figure 15C). The results showed that SELE, an adaptive immune gene, mainly regulates the TNF signalling pathway, cell adhesion molecules (CAMs) and fluid shear stress and atherosclerosis. Within the TNF signalling pathway, VCAM1 represents a specific type of Cell adhesion Molecule (CAM). Within Cell adhesion Molecules (CAMs), the adaptive immune gene ITGB2 regulates both *Staphylococcus aureus* infection and complement and coagulation cascades. From Figure 15C, we can see that F13A1 is mainly involved in the regulation of complement and coagulation cascades pathway. DEFB1, an innate immune-related gene, is mainly involved in the regulation of *S. aureus* infection and ABC transporters. Within *S. aureus* infection, other crosstalk genes such as KRT24 and FCGR2B also participate in the regulation. In addition, ITGB2 and other genes are associated with other pathways to regulate the immune function in both AD and PD. It can be inferred from the above that immune-related crosstalk genes interact with other genes and jointly influence the two diseases.

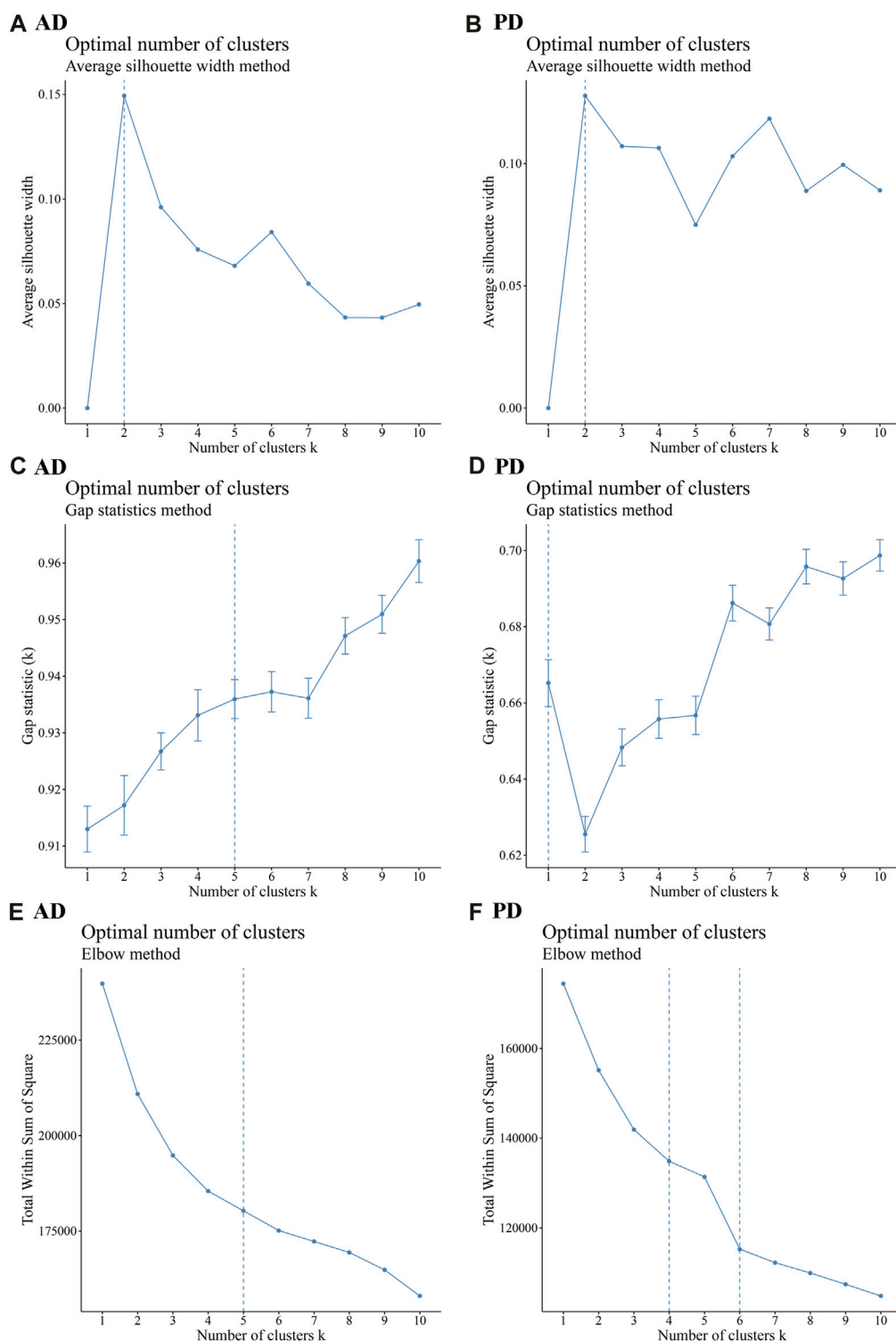


**FIGURE 9** Cluster number analysis using different methods (A–C) Average silhouette width, Gap statistic, and Elbow method to analyse the number of AD clusters; (D–F) Average silhouette width, Gap statistic, and Elbow method to analyse the number of PD clusters. The “ConsensusClusterPlus” R package was applied for cluster analysis.

## Discussion

The present bioinformatic study applied immunocorrelation analysis to identify immune-related genes, cells and pathways

that might serve as key linkage mechanisms between AD and PD. We found that innate immune cells M2 macrophages and NKT are highly expressed in both AD and PD. M2 macrophages are primarily involved in the Th2 immune response. Th2 cells produce

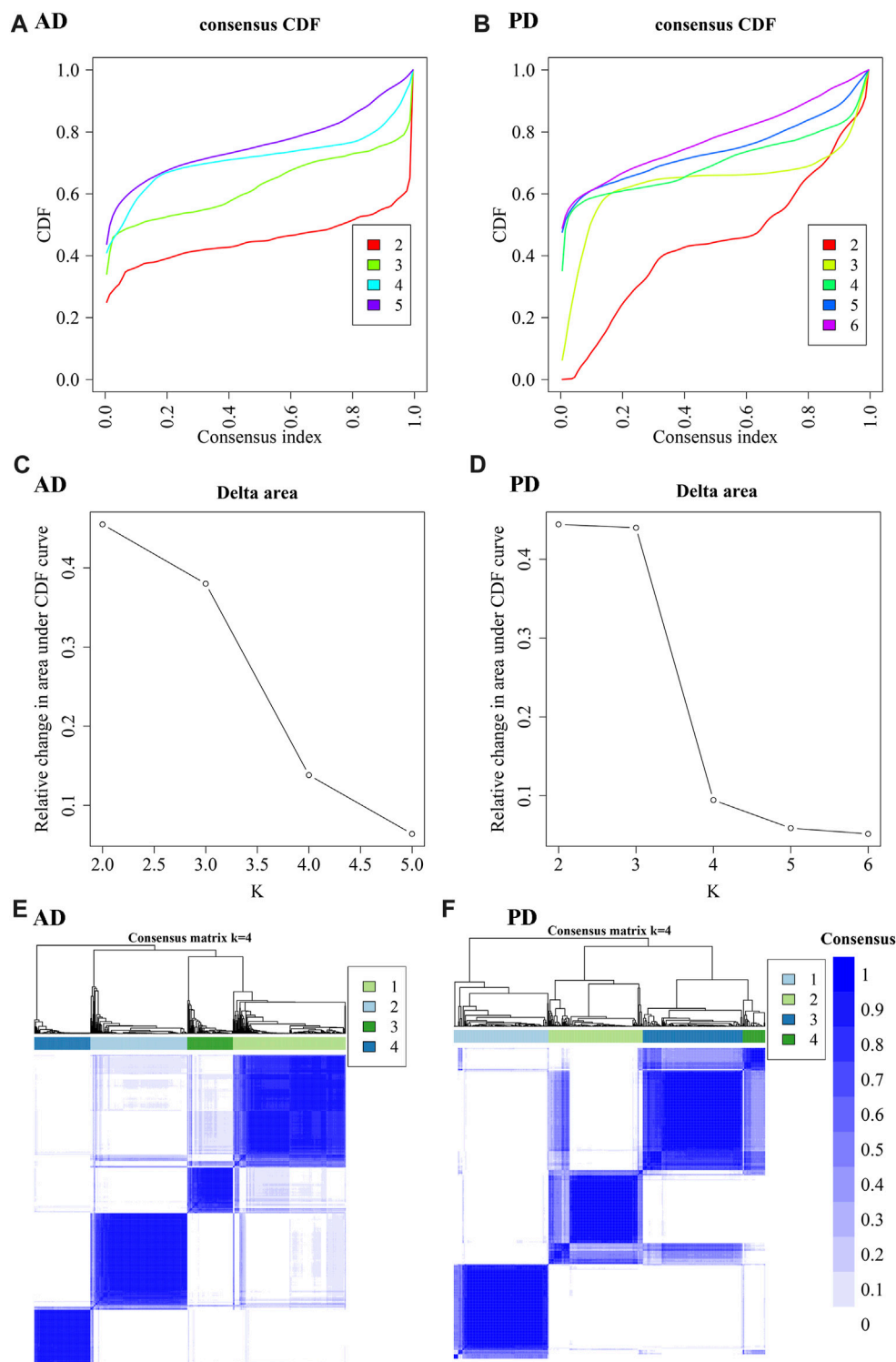
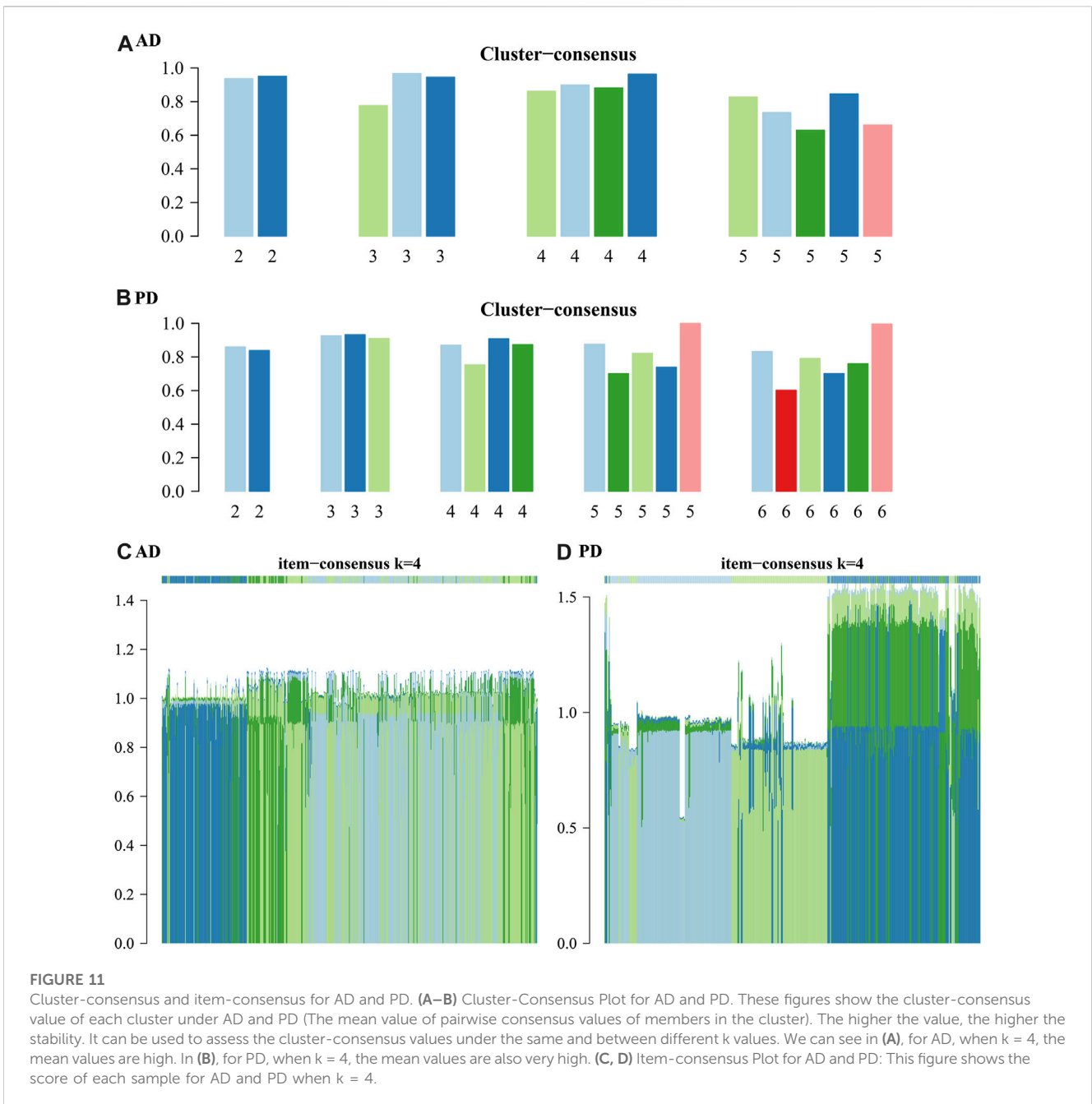


**FIGURE 10**

Cluster consistency analysis. **(A, B)** Consistent cumulative distribution function (CDF) plots for AD and PD. This figure shows the cumulative distribution function of scores with different values of  $K$ , which is used to determine the approximate maximum value of CDF for a selected  $k$  value, and the cluster analysis result that is the most reliable. That is, the  $k$  value with a small descending slope of CDF is considered. **(C, D)** Delta Area Plot of AD and PD: This figure shows the relative changes of areas under the CDF curve compared to  $k$  and  $k-1$ . When  $k = 2$ , since there is no  $k = 1$ , the first point represents the total area under the CDF curve at  $k = 2$  (that is, the area of the center line in Figure AB), rather than the relative change in area. **(E, F)** Consistent clustering diagram of AD and PD.



cytokines that promote the humoral immune response, including IL-4, IL-5, IL-6, IL-10 and IL-13 (Sun et al., 2021). NKT cells mediate proinflammatory and immunomodulatory effects, which range from B-cell regulation, production of specific antibodies, suppression of autoimmunity to cytokine production, dendritic cell crosstalk, and T/B cell interactions (Seidel et al., 2020a). Infiltration of the brain by peripheral NK cells with altered cytotoxic properties has been documented as a contributory mechanism to neuroinflammation in AD but the specific roles of infiltrating NKT cells, which share phenotypic and functional properties are less well understood in AD (Busse et al., 2021; Lu et al., 2021). In PD, NKT cells are known to be activated by several Gram-negative periodontal pathogens can play proinflammatory roles (Seidel et al., 2020b). Of note, gene expression based immune

cell infiltration analysis may include the extrapolation of certain genes that may also be expressed in non-immune cell lineages under conditions such as stress or inflammation, and this could account for the prediction of adipocytes and hepatocyte expression, which is unsupported by experimental evidence. For instance, ICAM-1, expressed on immune cell lineages, is overexpressed on adipocytes and hepatocytes (Farhood et al., 1995; Singh et al., 2023).

Among the adaptive immune cells, B-cells, CD4<sup>+</sup> memory T-cells and CD8<sup>+</sup> naive T-cells were found highly expressed in all 4 clusters of AD and PD. B cells might exert protective functions in periodontitis. B-cell-deficient mice show alveolar bone loss without bacterial infection, while clinical evidence shows that B cells and plasma cells, along with osteoclastogenic factors, are involved in alveolar bone destruction in periodontitis (Zouali, 2017). AD is

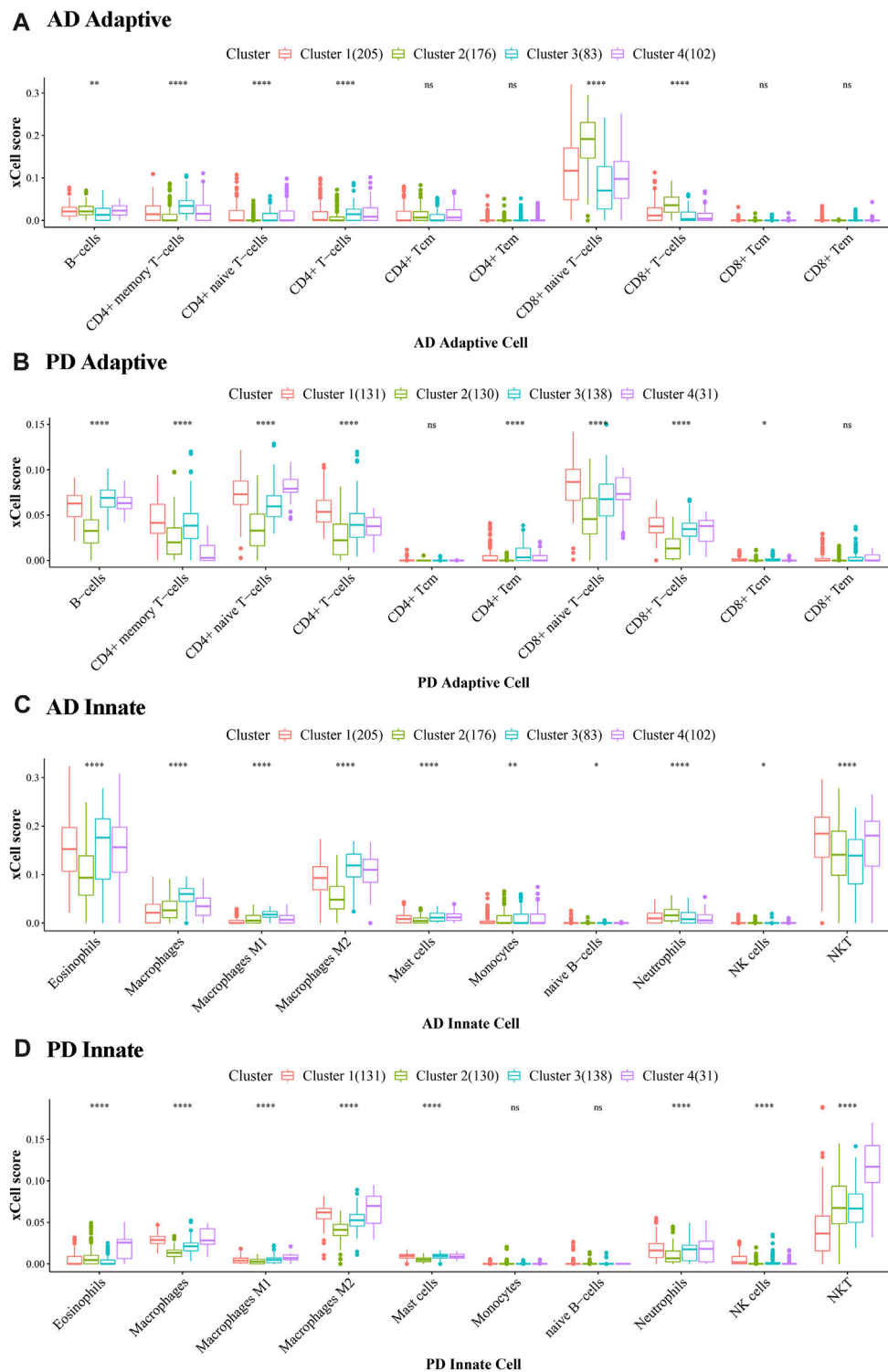


**FIGURE 12** Cluster level expression of Adaptive and Innate immune genes in AD and PD. (A, B) Adaptive immune gene expression in AD and PD. (C, D) Innate immune gene expression in AD and PD. ns:  $p > 0.05$ ; \*:  $p \leq 0.05$ ; \*\*:  $p \leq 0.01$ ; \*\*\*:  $p \leq 0.001$ ; \*\*\*\*:  $p \leq 0.0001$ . The xCell scores of Adaptive and Innate immune genes in AD and PD were compared using Kruskal-Wallis tests to test differences in scores of immune cells in different clusters.

associated with B cell accumulation in brain tissue which can produce IgG to induce microglial activation (Park et al., 2022). Experimental evidence supports the notion of infectious disease driven microglial activation in AD (Hao et al., 2022) along with

peripheral leukocyte infiltration of brain tissue secondary to persistent systemic inflammation (Lu et al., 2021), as seen in periodontitis, in particular NK cell infiltration (Le Page et al., 2018), and our findings were largely consistent. High levels of

TABLE 5 Significant immune cell populations in AD and PD.

|    |          | Adaptive immune cells top 3 |                                 |                                | Innate immune cells top 3 |                |     |
|----|----------|-----------------------------|---------------------------------|--------------------------------|---------------------------|----------------|-----|
| AD | cluster1 | B-cells                     | CD4 <sup>+</sup> memory T-cells | CD8 <sup>+</sup> naive T-cells | Eosinophils               | Macrophages M2 | NKT |
|    | cluster2 | B-cells                     | CD8 <sup>+</sup> T-cells        | CD8 <sup>+</sup> naive T-cells | Eosinophils               | Macrophages M2 | NKT |
|    | cluster3 | B-cells                     | CD4 <sup>+</sup> memory T-cells | CD8 <sup>+</sup> naive T-cells | Eosinophils               | Macrophages M2 | NKT |
|    | cluster4 | B-cells                     | CD4 <sup>+</sup> memory T-cells | CD8 <sup>+</sup> naive T-cells | Eosinophils               | Macrophages M2 | NKT |
| PD | cluster1 | B-cells                     | CD4 <sup>+</sup> memory T-cells | CD8 <sup>+</sup> naive T-cells | Macrophage                | Macrophages M2 | NKT |
|    | cluster2 | B-cells                     | CD4 <sup>+</sup> memory T-cells | CD8 <sup>+</sup> naive T-cells | Macrophage                | Macrophages M2 | NKT |
|    | cluster3 | B-cells                     | CD4 <sup>+</sup> memory T-cells | CD8 <sup>+</sup> naive T-cells | Macrophage                | Macrophages M2 | NKT |
|    | cluster4 | B-cells                     | CD4 <sup>+</sup> memory T-cells | CD8 <sup>+</sup> naive T-cells | Macrophage                | Macrophages M2 | NKT |

NKT cell-related immune genes were also implicated in AD in our results, and aberrant NKT cell homeostasis has been reported in AD (Sh et al., 2021). The CD8<sup>+</sup> naïve T cell subset was also overrepresented in AD samples, consistent with experimental evidence demonstrating CD8<sup>+</sup> T cell infiltration of AD-affected brain parenchyma which have been associated with upregulated IFN- $\beta$  signalling and infection (Altendorfer et al., 2022). Eosinophils were also markedly overrepresented, and eosinophilic inclusions are well documented in Alzheimer's neurofibrillary tangles (Qian et al., 2022). Eosinophilic signatures have also been inversely correlated with AD stage. The M2 macrophage signature noted in AD samples is corroborated by peripheral macrophage infiltration in experimental models of AD (Rentsendorj et al., 2018) and the M2 phenotype has been correlated with AD but not experimentally validated (Lin C. et al., 2022). M1/M2 phenotype switch is also a key feature of microglial changes in AD, and while *P. gingivalis* infection is associated with M1 type microglial switch, the stage of AD is an important determinant of M1/M2 microglial balance (Lin J. et al., 2022). Ageing and senescence are associated with deregulation of immune responses, and higher risk of both AD and PD. Furthermore, gender-based differences in AD pathology are recognised. A limitation of this investigation is that the datasets were not matched for age, gender, and disease stage which may induce confounding and should be addressed in future clinical investigations. Cluster analysis revealed innate immunity associated genes were comparatively highly expressed in cluster4 samples of AD and PD, and whether these samples represent a distinct phenotype, a later stage of disease progression, or represent more advanced age, begets further questions which should be dissected in future longitudinal studies to fully understand the PD-AD link.

Using a data mining approach with a series of reductive analyses, we obtained a 3 gene set, DUSP14, F13A1 and SELE, as key crosstalk genes linking PD and AD, which was largely supported by experimental and clinical data. The mechanistic role of DUSP14 in mediating AD and PD is not investigated but several DUSP genes are shown to be deregulated during AD pathogenesis (An et al., 2021). Targeting DUSP 14 can counter NLRP2 inflammasome mediated immune-inflammatory pathways and has shown positive effects in ameliorating neuroinflammation and cognitive dysfunction (Que et al., 2020). There are few reports regarding the roles of DUSP14 in the literature, mainly focusing on

pathways related to T cells. DUSP14 can downregulate T-cell receptor signalling by inhibiting TGF- $\beta$ -activated kinase 1-binding protein 1 (TAB1) activation (Yang et al., 2014). DUSP14 is a mitogen-activated protein kinase phosphatase that plays a critical role in the regulation of T cell activity. TRAF2 mediated Lys63-linked ubiquitination of DUSP14 leads to DUSP14 activation in T cells (Yang et al., 2016). DUSP14 directly interacts with TGF-beta-activated kinase 1 (TAK1)-binding protein 1 (TAB1) and dephosphorylated TAB1 at Ser(438), leading to TAB1-TAK1 complex inactivation in T cells and can downregulate T-cell receptor (TCR) signalling by inhibiting TAB1 activation (Yang et al., 2014). Activated DUSP14 also directly dephosphorylates extracellular signal-regulated kinases (ERK) and attenuates the ERK signalling pathway. TRAF2-mediated ubiquitination of Lys63-linked DUSP14 also enhances its phosphatase activity (Chen et al., 2019). Protein arginine methyltransferase (PRMT)5-mediated arginine methylation may sequentially stimulate TRAF2-mediated DUSP14 ubiquitination and phosphatase activity, leading to inhibition of TCR signalling (Yang et al., 2018). Therefore, enhancement/activation of DUSP14 or DUSP14 upstream molecules is a potential modality for the attenuation of autoimmune diseases such as systemic lupus erythematosus (SLE) (Chuang and Tan, 2019).

F13A1 is involved in clot stabilization and implicated in a number of immunoinflammatory diseases (Dull et al., 2021). The role of F13A1 has been investigated in AD. F13A1 subunit was detected by immunohistochemistry in a subset of AD reactive microglia, while F13A1 Val34Leu gene polymorphism is associated with sporadic AD where homozygous LL genotype shows about a fourfold higher risk of developing AD compared to the homozygous VV genotype (Gerardino et al., 2006). F13A1 may also influence the maintenance of neural connections (Festoff et al., 2001). The F13A1 204Phe allele is strongly associated with ischemic stroke in young women and the homozygous genotype (Phe/Phe) are associated with manifold higher stroke risk than heterozygous (Tyr/Phe) genotype (Pruissen et al., 2008). Functionally, a pro-angiogenic function of F13A1 is affected by the interaction between vascular endothelial growth factor receptor 2 (VEGFR2) and integrin  $\alpha\beta$ 3 on the cell membrane, which facilitates important steps in granulation tissue formation at wound sites. F13A1 deficiency can thus present as intracranial haemorrhage, delayed bleeding or chronic wounding of the skin and impaired

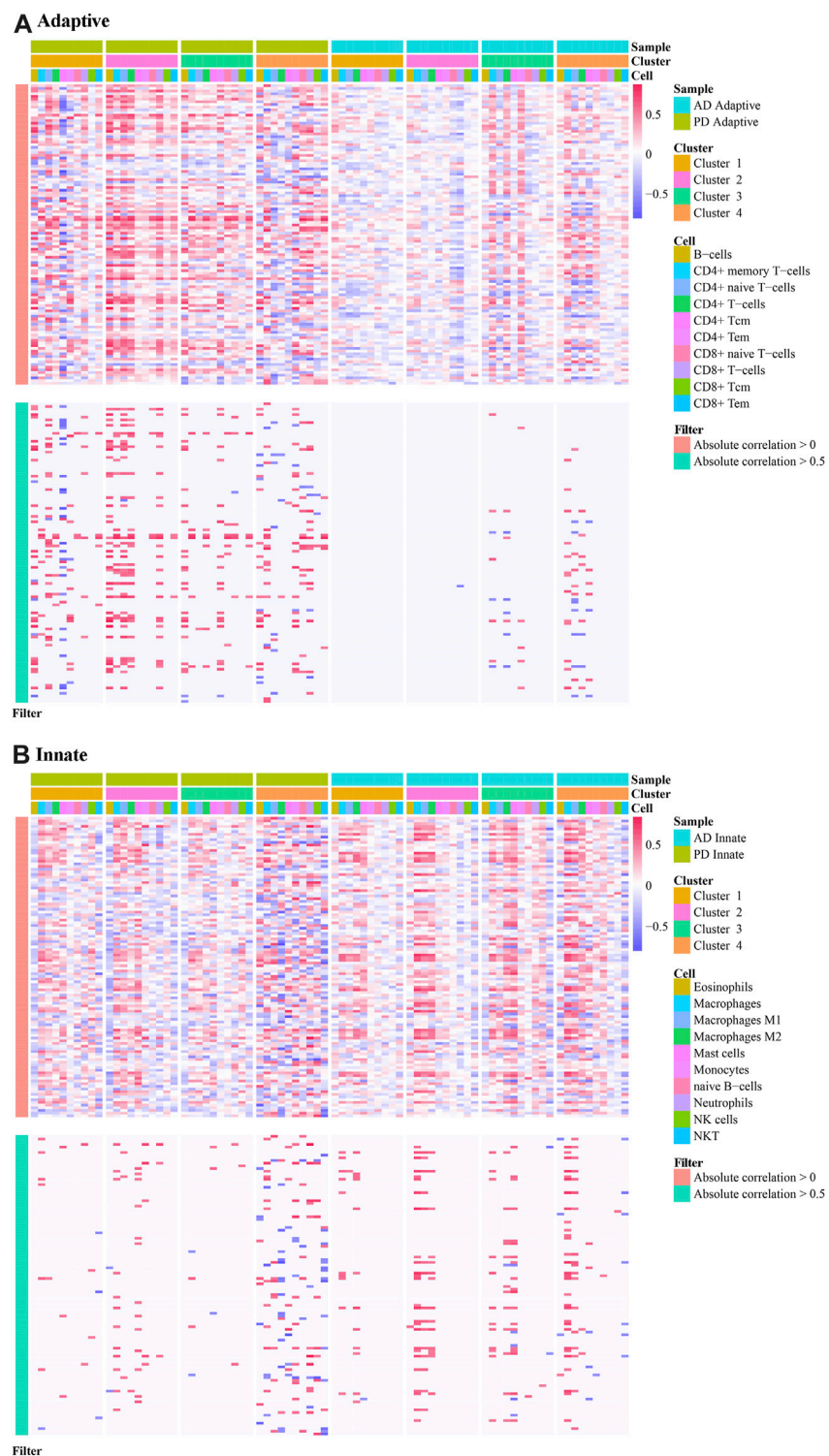


**FIGURE 13**

Correlation analysis applied to immune cell scores in different clusters. (A) The correlation of adaptive immune-related genes in different clusters in AD and PD; (B) The correlation of innate immune-related genes in different clusters in AD and PD. Spearman's correlation analysis was performed.

mucosal healing. F13A1 thus functions to link primary hemostasis, coagulation, and definitive tissue healing. Another important recently identified function of F13A1 is its ability to control cellular infiltration by binding to specific macromolecules,

thereby limiting bacterial spread at the wound site and promoting host cell migration and survival (Gemmati et al., 2016). In the brain, F13A1 expression has been detected by immunohistochemistry in reactive microglia during glioma

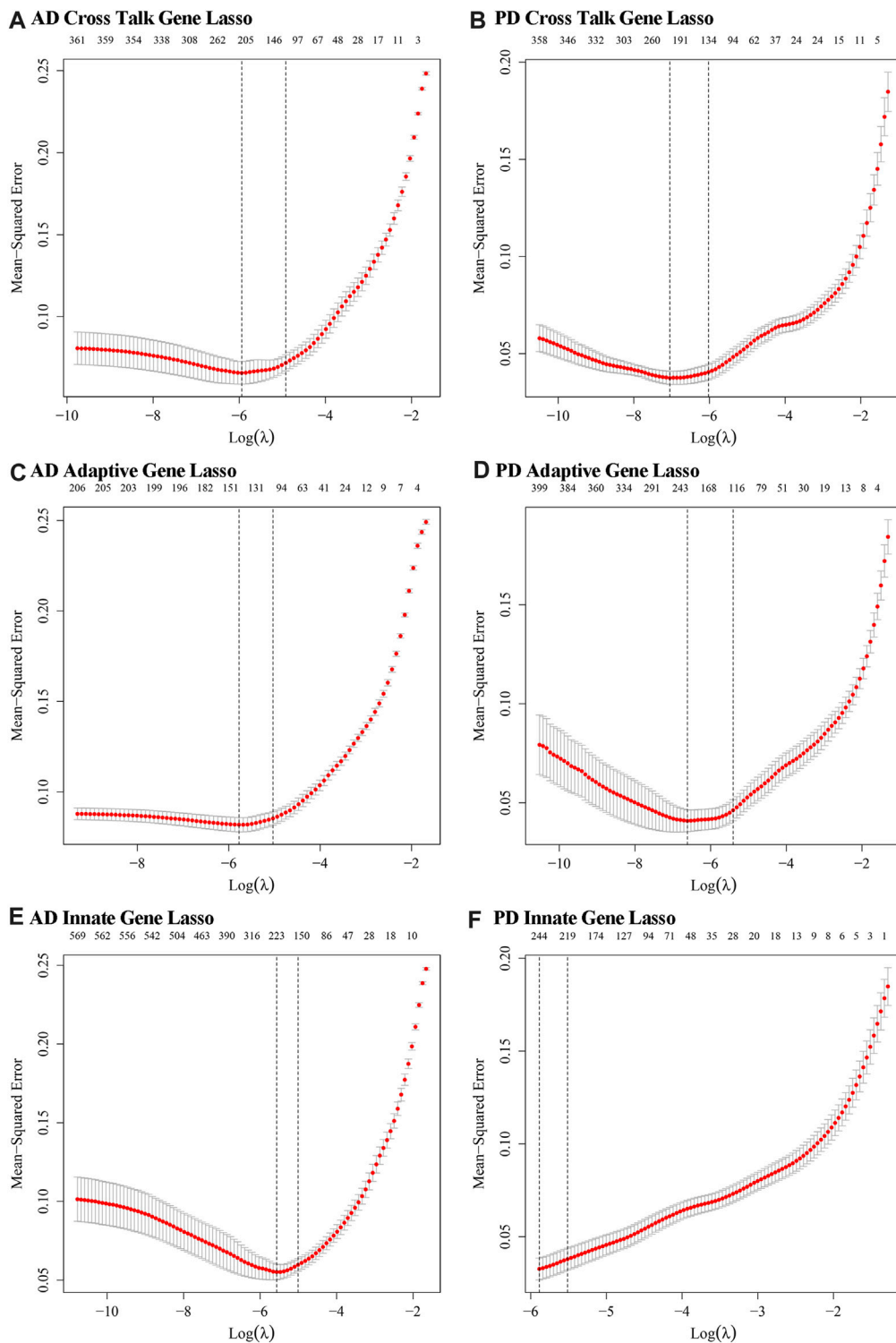
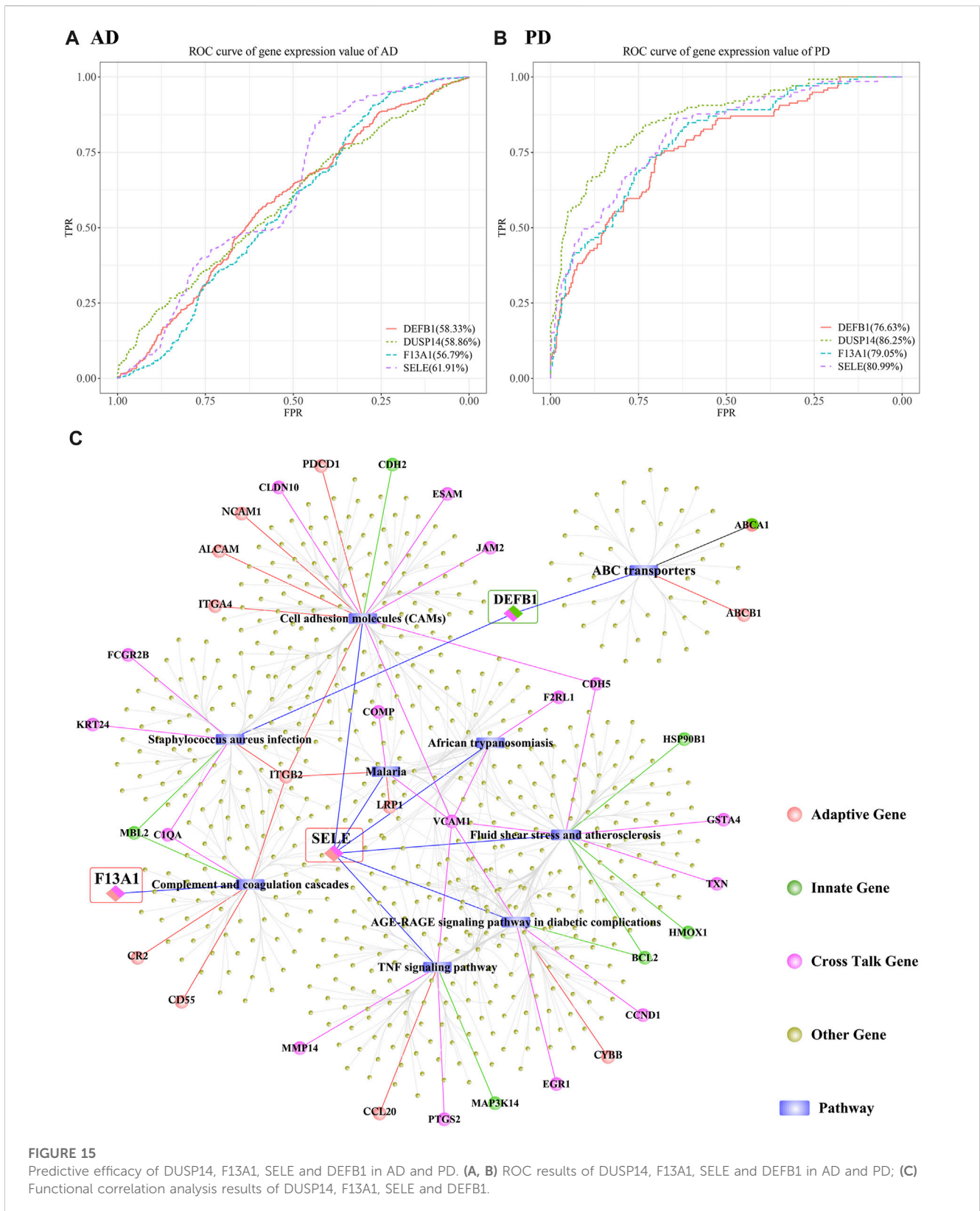


**FIGURE 14**

The optimal lambda values obtained from LASSO regression modelling of innate immune genes and adaptive immune genes. **(A, B)** Crosstalk genes: relationship between lambda value and mean square error in AD and PD Lasso regression analysis. The abscissa is log (lambda) and the ordinate is mean square error. There are two dashed lines in the figure, one is the value of  $\lambda$  with the minimum mean square error and the other is the value of  $\lambda$  with the standard error from the minimum mean square error. **(C, D)** Adaptive immune genes: lambda value and mean square error in AD and PD Lasso regression analysis. **(E, F)** Innate immune genes: lambda value and mean square error in AD and PD Lasso regression analysis.



formation, which is a distinctive feature of AD pathogenesis (Gerardino et al., 2006). F13A1 levels are gradually elevated from controls to mild cognitive impairment (MCI) and AD. More importantly, F13A1 in the serum proteome can serve as a

potential non-invasive early diagnostic marker of MCI and AD (Kang et al., 2016). Of note, PD pathogens can induce the upregulation of the coagulation cascade-related genes in endothelial cells (Salmina et al., 2010) and may contribute the

endothelial dysfunction inherent to AD pathogenesis (Hossain et al., 2020).

SELE encodes for E-selectin and is involved in Leukocyte/endothelial cell adhesion, and its expression is reported to increase 4-fold in *Treponema denticola* oral infections (Chukkapalli et al., 2014), a subgingival oral spirochete species which is a key periodontal pathogen (Zeng et al., 2021). Its role in several age-associated conditions such as age-related macular degeneration (Mullins et al., 2011) and other conditions. SELE has been found to be related with peripheral arterial occlusive disease (Shaker et al., 2010). The serum level of SELE has been found significantly elevated in systemic sclerosis with early onset disease (Hasegawa et al., 2014). Regarding periodontitis, the Ser128Arg polymorphism is associated with periodontitis (Houshmand et al., 2009). SELE expression is also found positively correlated with the duration of Sjogren's syndrome, characterised by dysregulation of circulating immune cells, T cells and antigen presenting cells and vascular endothelial extravasation (Turkcapar et al., 2005; Blochowiak et al., 2017). In an animal model of AD, SELE expression was found significantly elevated, indicating its role in AD development (Wang et al., 2020). The cell-surface glycoprotein E selectin plays an important role in immune adhesion (McEver, 2015). It is also associated with the accumulation of white blood cells at sites of inflammation by mediating cell adhesion to the intima of blood vessels. As a clinical diagnosis, AD shows variable pathology. Clinically, E-selectin has been found significantly raised in the cerebrospinal fluid (CSF) of AD patients without typical signature biomarker profiles, suggesting it may specifically mark the vascular mechanisms underlying AD pathology (Li et al., 2015). The SELE Ser128Arg gene polymorphism has also been associated with AD (Horstmann et al., 2010; Ribizzi et al., 2010; Flex et al., 2014) and SELE polymorphisms are also associated with Lewy body dementias (Rajkumar et al., 2020). The findings of the functional correlation analysis indicate an interaction between these candidate biomarker genes with key pathways intersecting adaptive immune responses, TNF alpha mediated inflammation, and endothelial dysfunction, supporting PD infection-mediated systemic immune dysregulation at the core of the AD-PD link.

Overall, the findings of this bioinformatic study were supported by existing experimental evidence addressing PD and AD but the roles of the discovered biomarkers DUSP14, F13A1 and SELE in mediating the link between the two diseases has not been addressed. A major limitation of the present study is the lack of validation experiments using cell, animal or clinical data. Therefore, the present data must be considered as a theoretical premise for further investigation that explores the validity of these biomarkers in large-scale clinical trials and their mechanistic roles in experimental or translational research focused on immune mechanisms implicated in AD and PD linkage.

## Conclusion

Bioinformatic analysis integrating experimental transcriptomic data from Alzheimer's disease and periodontitis revealed the most robust potentially shared molecular linkages. Three biomarker crosstalk genes; DUSP14, F13A1 and SELE were identified as the most robust signature.

Macrophages M2 and NKT among innate immune cells, and B-cells, CD4<sup>+</sup> memory T-cells and CD8<sup>+</sup> naive T-cells among adaptive immune cells emerged as top immune cells linking PD and AD. These findings warrant future research in experimental and clinical studies.

## Data availability statement

The datasets presented in this study can be found in online repositories. The names of the repository/repositories and accession number(s) can be found in the article/Supplementary Material.

## Ethics statement

Ethical approval was not required for the study involving humans in accordance with the local legislation and institutional requirements. Written informed consent to participate in this study was not required from the participants or the participants' legal guardians/next of kin in accordance with the national legislation and the institutional requirements.

## Author contributions

Conceptualization, XH and GS; methodology, JJ; software, MG, and MC; validation, JJ, YL, and LZ; formal analysis, BZ; investigation, MC; resources, JJ and MG; data curation, JJ and MG; writing—original draft preparation, JJ and MG; writing—review and editing, XH and GS; visualization, MG; supervision, XH; project administration, XH. All authors contributed to the article and approved the submitted version.

## Acknowledgments

We want to thank my colleagues for their collaboration and help during gathering data for my research project. We would also thank my parents and my lovely kid for their kindness to let me have time and energy to finish this work.

## Conflict of interest

The authors declare that the research was conducted in the absence of any commercial or financial relationships that could be construed as a potential conflict of interest.

## Publisher's note

All claims expressed in this article are solely those of the authors and do not necessarily represent those of their affiliated organizations, or those of the publisher, the editors and the reviewers. Any product that may be evaluated in this article, or claim that may be made by its manufacturer, is not guaranteed or endorsed by the publisher.

## References

- Agrawal, S., Baulch, J. E., Madan, S., Salah, S., Cheeks, S. N., Krattli, R. P., Jr., et al. (2022). Impact of IL-21-associated peripheral and brain crosstalk on the Alzheimer's disease neuropathology. *Cell Mol. Life Sci.* 79 (6), 331. doi:10.1007/s00018-022-04347-6
- Altendorfer, B., Unger, M. S., Poupardin, R., Hoog, A., Asslaber, D., Gratz, I. K., et al. (2022). Transcriptomic profiling identifies CD8+ T cells in the brain of aged and Alzheimer's disease transgenic mice as tissue-resident memory T cells. *J. Immunol.* 209 (7), 1272–1285. doi:10.4049/jimmunol.2100737
- An, N., Bassil, K., Al Jowf, G. I., Steinbusch, H. W., Rothermel, M., de Nijs, L., et al. (2021). Dual-specificity phosphatases in mental and neurological disorders. *Prog. Neurobiol.* 198, 101906. doi:10.1016/j.pneurobio.2020.101906
- Baima, G., Romandini, M., Citterio, F., Romano, F., and Aimetti, M. (2022). Periodontitis and accelerated biological aging: A geroscience approach. *J. Dent. Res.* 101 (2), 125–132. doi:10.1177/00220345211037977
- Bairamian, D., Sha, S., Rollion, N., Sokol, H., Dorothee, G., Lemere, C. A., et al. (2022). Microbiota in neuroinflammation and synaptic dysfunction: a focus on Alzheimer's disease. *Mol. Neurodegener.* 17 (1), 19. doi:10.1186/s13024-022-00522-2
- Bettcher, B. M., Tansey, M. G., Dorothee, G., and Heneka, M. T. (2021). Peripheral and central immune system crosstalk in Alzheimer disease - a research prospectus. *Nat. Rev. Neurol.* 17 (11), 689–701. doi:10.1038/s41582-021-00549-x
- Blochowiak, K. J., Olewicz-Gawlik, A., Trzybulska, D., Nowak-Gabryel, M., Kociecki, J., Witmanowski, H., et al. (2017). Serum ICAM-1, VCAM-1 and E-selectin levels in patients with primary and secondary Sjogren's syndrome. *Adv. Clin. Exp. Med.* 26 (5), 835–842. doi:10.17219/acem/61434
- Busse, S., Hoffmann, J., Michler, E., Hartig, R., Frodl, T., and Busse, M. (2021). Dementia-associated changes of immune cell composition within the cerebrospinal fluid. *Brain, Behav. Immunity-Health* 14, 100218. doi:10.1016/j.bbih.2021.100218
- Campbell, S. L., and Gear, C. W. (1995). The index of general nonlinear DAEs. *DAES. Numer. Math.* 72 (2), 173–196. doi:10.1007/s002110050165
- Charoentong, P., Finotello, F., Angelova, M., Mayer, C., Efreanova, M., Rieder, D., et al. (2017). Pan-cancer immunogenomic analyses reveal genotype-immunophenotype relationships and predictors of response to checkpoint blockade. *Cell Rep.* 18 (1), 248–262. doi:10.1016/j.celrep.2016.12.019
- Chen, H. F., Chuang, H. C., and Tan, T. H. (2019). Regulation of dual-specificity phosphatase (DUSP) ubiquitination and protein stability. *Int. J. Mol. Sci.* 20 (11), 2668. doi:10.3390/ijms20112668
- Chuang, H. C., and Tan, T. H. (2019). MAP4K family kinases and DUSP family phosphatases in T-cell signaling and systemic lupus erythematosus. *Cells* 8 (11), 1433. doi:10.3390/cells8111433
- Chukkapalli, S. S., Rivera, M. F., Velsko, I. M., Lee, J. Y., Chen, H., Zheng, D., et al. (2014). Invasion of oral and aortic tissues by oral spirochete *Treponema denticola* in ApoE(-/-) mice causally links periodontal disease and atherosclerosis. *Infect. Immun.* 82 (5), 1959–1967. doi:10.1128/IAI.01511-14
- Dioguardi, M., Crincoli, V., Laino, L., Alovise, M., Sovereto, D., Mastrangelo, F., et al. (2020). The role of periodontitis and periodontal bacteria in the onset and progression of Alzheimer's disease: a systematic review. *J. Clin. Med.* 9 (2), 495. doi:10.3390/jcm9020495
- Dominy, S. S., Lynch, C., Ermini, F., Benedyk, M., Marczyk, A., Konradi, A., et al. (2019). Porphyromonas gingivalis in Alzheimer's disease brains: evidence for disease causation and treatment with small-molecule inhibitors. *Sci. Adv.* 5 (1), eaau3333. doi:10.1126/sciadv.aau3333
- Dull, K., Fazekas, F., and Töröcsik, D. (2021). Factor XIII-A in diseases: role beyond blood coagulation. *Int. J. Mol. Sci.* 22 (3), 1459. doi:10.3390/ijms22031459
- Eriksson, U. K., Pedersen, N. L., Reynolds, C. A., Hong, M. G., Prince, J. A., Gatz, M., et al. (2011). Associations of gene sequence variation and serum levels of C-reactive protein and interleukin-6 with Alzheimer's disease and dementia. *J. Alzheimers Dis.* 23 (2), 361–369. doi:10.3233/JAD-2010-101671
- Farhood, A., McGuire, G. M., Manning, A. M., Miyasaka, M., Smith, C. W., and Jaeschke, H. (1995). Interleukin-1 (ICAM-1) expression and its role in neutrophil-induced ischemia-reperfusion injury in rat liver. *J. Leucocyte Biol.* 57 (3), 368–374. doi:10.1002/jlb.57.3.368
- Festoff, B. W., Suo, Z., and Citron, B. A. (2001). Plasticity and stabilization of neuromuscular and CNS synapses: interactions between thrombin protease signaling pathways and tissue transglutaminase. *Int. Rev. Cytol.* 211, 153–177. doi:10.1016/s0074-7696(01)11018-1
- Flex, A., Giovannini, S., Biscetti, F., Liperoti, R., Spalletta, G., Straface, G., et al. (2014). Effect of proinflammatory gene polymorphisms on the risk of Alzheimer's disease. *Neurodegener. Dis.* 13 (4), 230–236. doi:10.1159/000353395
- Gaudilliere, D. K., Culos, A., Djebali, K., Tsai, A. S., Ganio, E. A., Choi, W. M., et al. (2019). Systemic immunologic consequences of chronic periodontitis. *J. Dent. Res.* 98 (9), 985–993. doi:10.1177/0022034519857714
- Gemmati, D., Vigliano, M., Burini, F., Mari, R., El Mohsein, H. H., Parmeggiani, F., et al. (2016). Coagulation factor XIIIa (F13A1): novel perspectives in treatment and pharmacogenetics. *Curr. Pharm. Des.* 22 (11), 1449–1459. doi:10.2174/1381612822666151210122954
- Gerardino, L., Papaleo, P., Flex, A., Gaetani, E., Fioroni, G., Pola, P., et al. (2006). Coagulation factor XIII Val34Leu gene polymorphism and Alzheimer's disease. *Neurol. Res.* 28 (8), 807–809. doi:10.1179/016164106X110454
- Hajishengallis, G. (2014b). Aging and its impact on innate immunity and inflammation: implications for periodontitis. *J. Oral Biosci.* 56 (1), 30–37. doi:10.1016/j.job.2013.09.001
- Hajishengallis, G. (2014a). The inflammophilic character of the periodontitis-associated microbiota. *Mol. Oral Microbiol.* 29 (6), 248–257. doi:10.1111/omi.12065
- Hao, X., Li, Z., Li, W., Katz, J., Michalek, S. M., Barnum, S. R., et al. (2022). Periodontal infection aggravates C1q-mediated microglial activation and synapse pruning in Alzheimer's mice. *Front. Immunol.* 13, 816640. doi:10.3389/fimmu.2022.816640
- Hasegawa, M., Asano, Y., Endo, H., Fujimoto, M., Goto, D., Ihn, H., et al. (2014). Serum adhesion molecule levels as prognostic markers in patients with early systemic sclerosis: a multicentre, prospective, observational study. *PLoS One* 9 (2), e88150. doi:10.1371/journal.pone.0088150
- Holmes, C., Cunningham, C., Zotova, E., Culliford, D., and Perry, V. H. (2011). Proinflammatory cytokines, sickness behavior, and Alzheimer disease. *Neurology* 77 (3), 212–218. doi:10.1212/WNL.0b013e318225ae07
- Horstmann, S., Budig, L., Gardner, H., Koziol, J., Deuschle, M., Schilling, C., et al. (2010). Matrix metalloproteinases in peripheral blood and cerebrospinal fluid in patients with Alzheimer's disease. *Int. Psychogeriatr.* 22 (6), 966–972. doi:10.1017/S1041610210000827
- Hossain, K. H., Okamoto, T., Usuda, H., Jahan, I., Niibayashi, T., and Wada, K. (2020). Differential expression of pro-inflammatory and pro-coagulant genes in endothelial cells induced by Porphyromonas gingivalis lipopolysaccharide, Escherichia coli lipopolysaccharide, and zymosan. *Shimane J. Med. Sci.* 37 (4), 123–132. doi:10.51010/sjms.37.4\_123
- Houshmand, B., Rafiei, A., Hajilooi, M., Mani-Kashani, K., and Gholami, L. (2009). E-selectin and L-selectin polymorphisms in patients with periodontitis. *J. Periodontol. Res.* 44 (1), 88–93. doi:10.1111/j.1600-0765.2008.01092.x
- Hu, X., Zhang, J., Qiu, Y., and Liu, Z. (2021). Periodontal disease and the risk of Alzheimer's disease and mild cognitive impairment: a systematic review and meta-analysis. *Psychogeriatrics* 21 (5), 813–825. doi:10.1111/psyg.12743
- Kang, S., Jeong, H., Baek, J. H., Lee, S. J., Han, S. H., Cho, H. J., et al. (2016). PiB-PET imaging-based serum proteome profiles predict mild cognitive impairment and Alzheimer's disease. *J. Alzheimers Dis.* 53 (4), 1563–1576. doi:10.3233/JAD-160025
- Kinney, J. W., Bemiller, S. M., Murtishaw, A. S., Leisgang, A. M., Salazar, A. M., and Lamb, B. T. (2018). Inflammation as a central mechanism in Alzheimer's disease. *Alzheimers Dement. (N Y)* 4, 575–590. doi:10.1016/j.trci.2018.06.014
- Le Page, A., Dupuis, G., Frost, E. H., Larbi, A., Pawelec, G., Witkowski, J. M., et al. (2018). Role of the peripheral innate immune system in the development of Alzheimer's disease. *Exp. Gerontol.* 107, 59–66. doi:10.1016/j.exger.2017.12.019
- Li, G., Xiong, K., Korff, A., Pan, C., Quinn, J. F., Galasko, D. R., et al. (2015). Increased CSF E-selectin in clinical Alzheimer's disease without altered CSF A $\beta$ 42 and tau. *J. Alzheimers Dis.* 47 (4), 883–887. doi:10.3233/JAD-150420
- Lin, C., Xu, C., Zhou, Y., Chen, A., and Jin, B. (2022a). Identification of biomarkers related to M2 macrophage infiltration in Alzheimer's disease. *Cells* 11 (15), 2365. doi:10.3390/cells11152365
- Lin, J., Huang, D., Xu, H., Zhan, F., and Tan, X. (2022b). Macrophages: A communication network linking Porphyromonas gingivalis infection and associated systemic diseases. *Front. Immunol.* 13, 952040. doi:10.3389/fimmu.2022.952040
- Lopez-Rodriguez, A. B., Hennessy, E., Murray, C. L., Nazmi, A., Delaney, H. J., Healy, D., et al. (2021). Acute systemic inflammation exacerbates neuroinflammation in Alzheimer's disease: IL-1 $\beta$  drives amplified responses in primed astrocytes and neuronal network dysfunction. *Alzheimers Dement.* 17 (10), 1735–1755. doi:10.1002/alz.12341
- Lu, Y., Li, K., Hu, Y., and Wang, X. (2021). Expression of immune related genes and possible regulatory mechanisms in Alzheimer's disease. *Front. Immunol.* 12, 768966. doi:10.3389/fimmu.2021.768966
- Maekawa, T., Krauss, J. L., Abe, T., Jotwani, R., Triantafyllou, M., Triantafyllou, K., et al. (2014). Porphyromonas gingivalis manipulates complement and TLR signaling to uncouple bacterial clearance from inflammation and promote dysbiosis. *Cell Host Microbe* 15 (6), 768–778. doi:10.1016/j.chom.2014.05.012
- McEver, R. P. (2015). Selectins: initiators of leucocyte adhesion and signalling at the vascular wall. *Cardiovasc Res.* 107 (3), 331–339. doi:10.1093/cvr/cvv154
- McManus, R. M., Mills, K. H., and Lynch, M. A. (2015). T cells-protective or pathogenic in Alzheimer's disease? *J. Neuroimmunol. Pharmacol.* 10 (4), 547–560. doi:10.1007/s11481-015-9612-2
- Mullins, R. F., Skeie, J. M., Folk, J. C., Solivan-Timpe, F. M., Oetting, T. A., Huang, J., et al. (2011). Evaluation of variants in the selectin genes in age-related macular degeneration. *BMC Med. Genet.* 12, 58. doi:10.1186/1471-2350-12-58

- Murakami, S., Mealey, B. L., Mariotti, A., and Chapple, I. L. C. (2018). Dental plaque-induced gingival conditions. *J. Periodontol.* 89 (1), S17–S27–S27. doi:10.1002/JPER.17-0095
- Park, J. C., Noh, J., Jang, S., Kim, K. H., Choi, H., Lee, D., et al. (2022). Association of B cell profile and receptor repertoire with the progression of Alzheimer's disease. *Cell Rep.* 40 (12), 111391. doi:10.1016/j.celrep.2022.111391
- Pruissen, D. M., Slooter, A. J., Rosendaal, F. R., van der Graaf, Y., and Algra, A. (2008). Coagulation factor XIII gene variation, oral contraceptives, and risk of ischemic stroke. *Blood* 111 (3), 1282–1286. doi:10.1182/blood-2007-08-110254
- Puris, E., Auriola, S., Korhonen, P., Loppi, S., Kanninen, K. M., Malm, T., et al. (2021). Systemic inflammation induced changes in protein expression of ABC transporters and ionotropic glutamate receptor subunit 1 in the cerebral cortex of familial Alzheimer's disease mouse model. *J. Pharm. Sci.* 110 (12), 3953–3962. doi:10.1016/j.xphs.2021.08.013
- Qian, X. H., Liu, X. L., Chen, S. D., and Tang, H. D. (2022). Identification of immune hub genes associated with Braak stages in Alzheimer's Disease and their correlation of immune infiltration. *Front. Aging Neurosci.* 14, 887168. doi:10.3389/fgene.2022.887168
- Que, Y. Y., Zhu, T., Zhang, F. X., and Peng, J. (2020). Neuroprotective effect of DUSP14 overexpression against isoflurane-induced inflammatory response, pyroptosis and cognitive impairment in aged rats through inhibiting the NLRP3 inflammasome. *Eur. Rev. Med. Pharmacol. Sci.* 24 (12), 7101–7113. doi:10.26355/eurrev\_202006\_21704
- Rajkumar, A. P., Bidkhorji, G., Shoaie, S., Clarke, E., Morrin, H., Hye, A., et al. (2020). Postmortem cortical transcriptomics of Lewy body dementia reveal mitochondrial dysfunction and lack of neuroinflammation. *Am. J. Geriatr. Psychiatry* 28 (1), 75–86. doi:10.1016/j.jagp.2019.06.007
- Rakic, S., Hung, Y. M. A., Smith, M., So, D., Tayler, H. M., Varney, W., et al. (2018). Systemic infection modifies the neuroinflammatory response in late stage Alzheimer's disease. *Acta Neuropathol. Commun.* 6 (1), 88. doi:10.1186/s40478-018-0592-3
- Rentsendorj, A., Sheyn, J., Fuchs, D. T., Daley, D., Salumbides, B. C., Schubloom, H. E., et al. (2018). A novel role for osteopontin in macrophage-mediated amyloid- $\beta$  clearance in Alzheimer's models. *Brain, Behav. Immun.* 67, 163–180. doi:10.1016/j.bbi.2017.08.019
- Ribizzi, G., Fiordoro, S., Barocci, S., Ferrari, E., and Megna, M. (2010). Cytokine polymorphisms and Alzheimer disease: possible associations. *Neurol. Sci.* 31 (3), 321–325. doi:10.1007/s10072-010-0221-9
- Ryder, M. I. (2020). Porphyromonas gingivalis and Alzheimer disease: recent findings and potential therapies. *J. Periodontology* 91, S45–S49–S49. doi:10.1002/JPER.20-0104
- Salmina, A. B., Inzhutova, A. I., Malinovskaya, N. A., and Petrova, M. M. (2010). Endothelial dysfunction and repair in Alzheimer-type neurodegeneration: neuronal and glial control. *J. Alzheimer's Dis.* 22 (1), 17–36. doi:10.3233/JAD-2010-091690
- Seidel, A., Seidel, C. L., Weider, M., Junker, R., Golz, L., and Schmetzer, H. (2020a). Influence of natural killer cells and natural killer T cells on periodontal disease: A systematic review of the current literature. *Int. J. Mol. Sci.* 21 (24), 9766. doi:10.3390/ijms21249766
- Seidel, A., Seidel, C. L., Weider, M., Junker, R., Gözl, L., and Schmetzer, H. (2020b). Influence of natural killer cells and natural killer T cells on periodontal disease: A systematic review of the current literature. *Int. J. Mol. Sci.* 21 (24), 9766. doi:10.3390/ijms21249766
- Sh, Y., Liu, B., Zhang, J., Zhou, Y., Hu, Z., and Zhang, X. (2021). Application of artificial intelligence modeling technology based on fluid biopsy to diagnose Alzheimer's disease. *Front. Aging Neurosci.* 13, 768229. doi:10.3389/fgene.2021.768229
- Shaker, O., Zahra, A., Sayed, A., Refaat, A., El-Khaiat, Z., Hegazy, G., et al. (2010). Role of ICAM-1 and E-selectin gene polymorphisms in pathogenesis of PAOD in Egyptian patients. *Vasc. Health Risk Manag.* 6, 9–15. doi:10.2147/vhrm.s8143
- Shen, X. N., Niu, L. D., Wang, Y. J., Cao, X. P., Liu, Q., Tan, L., et al. (2019). Inflammatory markers in Alzheimer's disease and mild cognitive impairment: a meta-analysis and systematic review of 170 studies. *J. Neurol. Neurosurg. Psychiatry* 90 (5), 590–598. doi:10.1136/jnnp-2018-319148
- Singh, V., Kaur, R., Kumari, P., Pasricha, C., and Singh, R. (2023). ICAM-1 and VCAM-1: gatekeepers in various inflammatory and cardiovascular disorders. *Clin. Chim. Acta* 548, 117487. doi:10.1016/j.cca.2023.117487
- Sun, X., Gao, J., Meng, X., Lu, X., Zhang, L., and Chen, R. (2021). Polarized macrophages in periodontitis: characteristics, function, and molecular signaling. *Front. Immunol.* 12, 763334. doi:10.3389/fimmu.2021.763334
- Tao, Q., Ang, T. F. A., DeCarli, C., Auerbach, S. H., Devine, S., Stein, T. D., et al. (2018). Association of chronic low-grade inflammation with risk of Alzheimer disease in ApoE4 carriers. *JAMA Netw. Open* 1 (6), e183597. doi:10.1001/jamanetworkopen.2018.3597
- Turkcapar, N., Sak, S. D., Saatci, M., Duman, M., and Olmez, U. (2005). Vasculitis and expression of vascular cell adhesion molecule-1, intercellular adhesion molecule-1, and E-selectin in salivary glands of patients with Sjogren's syndrome. *J. Rheumatol.* 32 (6), 1063–1070.
- van Olst, L., Coenen, L., Nieuwland, J. M., Rodriguez-Mogeda, C., de Wit, N. M., Kamerlings, A., et al. (2022). Crossing borders in Alzheimer's disease: A T cell's perspective. *Adv. Drug Deliv. Rev.* 188, 114398. doi:10.1016/j.addr.2022.114398
- Walker, K. A., Gross, A. L., Moghekar, A. R., Soldan, A., Pettigrew, C., Hou, X., et al. (2020). Association of peripheral inflammatory markers with connectivity in large-scale functional brain networks of non-demented older adults. *Brain Behav. Immun.* 87, 388–396. doi:10.1016/j.bbi.2020.01.006
- Wang, Y., Zhang, X., Song, Q., Hou, Y., Liu, J., Sun, Y., et al. (2020). Characterization of the chromatin accessibility in an Alzheimer's disease (AD) mouse model. *Alzheimers Res. Ther.* 12 (1), 29. doi:10.1186/s13195-020-00598-2
- Xie, J., Gorle, N., Vandendriessche, C., Van Imschoot, G., Van Wouterghem, E., Van Cauwenbergh, C., et al. (2021). Low-grade peripheral inflammation affects brain pathology in the App(NL-G-F) mouse model of Alzheimer's disease. *Acta Neuropathol. Commun.* 9 (1), 163. doi:10.1186/s40478-021-01253-z
- Xu, X. W., Liu, X., Shi, C., and Sun, H. C. (2021). Roles of immune cells and mechanisms of immune responses in periodontitis. *Chin. J. Dent. Res.* 24 (4), 219–230. doi:10.3290/j.cjdr.b2440547
- Yang, C. Y., Chiu, L. L., Chang, C. C., Chuang, H. C., and Tan, T. H. (2018). Induction of DUSP14 ubiquitination by PRMT5-mediated arginine methylation. *FASEB J.* 32, fj201800244RR. doi:10.1096/fj.201800244RR
- Yang, C. Y., Chiu, L. L., and Tan, T. H. (2016). TRAF2-mediated Lys63-linked ubiquitination of DUSP14/MKP6 is essential for its phosphatase activity. *Cell Signal* 28 (1), 145–151. doi:10.1016/j.cellsig.2015.10.017
- Yang, C. Y., Li, J. P., Chiu, L. L., Lan, J. L., Chen, D. Y., Chuang, H. C., et al. (2014). Dual-specificity phosphatase 14 (DUSP14/MKP6) negatively regulates TCR signaling by inhibiting TAB1 activation. *J. Immunol.* 192 (4), 1547–1557. doi:10.4049/jimmunol.1300989
- Zeng, H., Chan, Y., Gao, W., Leung, W. K., and Watt, R. M. (2021). Diversity of Treponema denticola and other oral treponeme lineages in subjects with periodontitis and gingivitis. *Microbiol. Spectr.* 9 (2), e0070121. doi:10.1128/Spectrum.00701-21
- Zouali, M. (2017). The emerging roles of B cells as partners and targets in periodontitis. *Autoimmunity* 50 (1), 61–70. doi:10.1080/08916934.2016.1261841